

# UCSF

## UC San Francisco Previously Published Works

### Title

Connective Tissue Growth Factor Regulates Retinal Neovascularization through p53 Protein-dependent Transactivation of the Matrix Metalloproteinase (MMP)-2 Gene\*

### Permalink

<https://escholarship.org/uc/item/36p841mj>

### Journal

Journal of Biological Chemistry, 287(48)

### ISSN

0021-9258

### Authors

Chintala, Hembindu  
Liu, Haibo  
Parmar, Rahul  
[et al.](#)

### Publication Date

2012-11-01

### DOI

10.1074/jbc.m112.386565

Peer reviewed

# Connective Tissue Growth Factor Regulates Retinal Neovascularization through p53 Protein-dependent Transactivation of the Matrix Metalloproteinase (MMP)-2 Gene<sup>\*[5]</sup>

Received for publication, May 30, 2012, and in revised form, September 19, 2012. Published, JBC Papers in Press, October 9, 2012, DOI 10.1074/jbc.M112.386565

Hembindu Chintala<sup>‡</sup>, Haibo Liu<sup>‡</sup>, Rahul Parmar<sup>‡</sup>, Monika Kamalska<sup>‡</sup>, Yoon Ji Kim<sup>‡</sup>, David Lovett<sup>§</sup>, Maria B. Grant<sup>¶</sup>, and Brahim Chaqour<sup>¶||1</sup>

From the <sup>‡</sup>State University of New York Eye Institute and Departments of Cell Biology and <sup>||</sup>Ophthalmology, State University of New York Downstate Medical Center, Brooklyn, New York 11203, the <sup>§</sup>San Francisco Veterans Affairs Medical Center, University of California, San Francisco, California 94121, and the <sup>¶</sup>Departments of Pharmacology and Therapeutics, University of Florida, Gainesville, Florida 32610

**Background:** The role of connective tissue growth factor (CTGF/CCN2) in pathological angiogenesis in the retina is unknown.

**Results:** CTGF/CCN2 stimulates retinal neovascularization through transactivation of p53 target genes such as matrix metalloproteinase (MMP)-2.

**Conclusion:** CTGF/CCN2 effects on abnormal vessel formation in the retina are mediated by p53 and MMP-2.

**Significance:** CTGF/CCN2 and its downstream effectors are potential targets in the development of new antiangiogenic treatments.

Pathological angiogenesis in the retina is driven by dysregulation of hypoxia-driven stimuli that coordinate physiological vessel growth. How the various components of the neovascularization signaling network are integrated to yield pathological changes has not been defined. Connective tissue growth factor (CTGF/CCN2) is an inducible matricellular protein that plays a major role in fibroproliferative disorders. Here, we show that CTGF/CCN2 was dynamically expressed in the developing murine retinal vasculature and was abnormally increased and localized within neovascular tufts in the mouse eye with oxygen-induced retinopathy. Consistent with its propitious vascular localization, ectopic expression of the *CTGF/CCN2* gene further accelerated neovascularization, whereas lentivirus-mediated loss-of-function or -expression of *CTGF/CCN2* harnessed ischemia-induced neovessel outgrowth in oxygen-induced retinopathy mice. The neovascular effects of CTGF/CCN2 were mediated, at least in part, through increased expression and activity of matrix metalloproteinase (MMP)-2, which drives vascular remodeling through degradation of matrix and non matrix proteins, migration and invasion of endothelial cells, and formation of new vascular patterns. In cultured cells, CTGF/CCN2 activated the *MMP-2* promoter through increased expression and tethering of the p53 transcription factor to a highly conserved p53-binding sequence within the *MMP-2* promoter. Concordantly, the neovascular effects of CTGF/CCN2 were suppressed

by p53 inhibition that culminated in reduced enrichment of the *MMP-2* promoter with p53 and decreased *MMP-2* gene expression. Our data identified new gene targets and downstream effectors of CTGF/CCN2 and provided the rational basis for targeting the p53 pathway to curtail the effects of CTGF/CCN2 on neovessel formation associated with ischemic retinopathy.

The most common diseases responsible for vision impairment and new onset blindness are due to retinal vascular/capillary damage and/or abnormalities of retinal or choroidal neovascularization (1, 2). Such alterations occur in diabetic retinopathy, age-related macular degeneration, central retinal vein occlusion, and retinopathy of prematurity (1). These conditions can result in intraocular hemorrhage and tractional retinal detachment leading to severe visual loss. In particular, retinopathy of prematurity, which is a leading cause of visual impairment in low birth weight infants in developed countries, is initiated by delayed retinal vascular growth and insufficient vascularization after premature birth (3). The ensuing retinal ischemia triggers the release of angiogenic factors that promote formation of abnormal neovessels that break through the inner limiting membrane into the vitreous (4). Prevention of neovessel growth is a promising strategy of intervention to improve long term prognosis of visual outcome and quality of life for many patients.

Physiologically, the retinal circulation is supported by the central retinal artery branching to superficial arteries, which dive into the retina to form a dense network of capillaries in the deeper retinal layers. Unlike the choroidal circulation, which is controlled by sympathetic innervation and supplies the outer part of the retina, the retinal circulation has no autonomic innervation and is controlled by local factors. The expression or

\* This work was supported, in whole or in part, by National Institutes of Health Grants EY022091-01 and EY019387-01A1 (to B. C.) and DK39776 (to D. L.) from NEI.

[5] This article contains supplemental Fig. 1.

<sup>1</sup> To whom correspondence should be addressed: SUNY Eye Institute, Depts. of Cell Biology and Ophthalmology, SUNY Downstate Medical Center, 450 Clarkson Ave., Box 5, Brooklyn, NY 11203. Tel.: 718-270-8285; Fax: 718-270-3732; E-mail: bchaqour@downstate.edu.

lack thereof of multiple blood- and/or stroma-derived cytokines and chemokines, including the vascular endothelial growth factor (VEGF), insulin-like growth factor, platelet-derived growth factor (PDGF), and angiopoietin systems, has been implicated in dysregulation of growth, migration, adhesion, and differentiation of retinal vascular cells in retinal vascular diseases (5, 6). Interestingly, an unusual signaling system with profound effects on vascular development has emerged from the study of a subset of extracellular matrix (ECM)<sup>2</sup> proteins known as cysteine-rich protein 61/connective tissue growth factor/novel overexpressed (CCN). Cyr61/CCN1 and CTGF/CCN2, the most functionally prominent members of the CCN family, share ~56% amino acid sequence homology and a typical multimodular organization characteristic of most ECM proteins (7, 8). Both proteins are encoded by immediate early genes that are sensitive to regulation by a myriad of chemical and mechanical stimuli, including serum growth factors, inflammatory cytokines, hypoxia, and mechanical strain (9–13). Functionally, both proteins exhibit distinct and overlapping biological roles as they bind many of the same integrin and growth factor receptors and ECM proteins and function through similar signal transduction mechanisms to regulate various biological processes (14–18). However, the specific biological effects of Cyr61/CCN1 and CTGF/CCN2 are cell type- and context-dependent and at times antithetic to one another. In particular, our studies have shown that Cyr61/CCN1 enhanced physiological adaptation of the retinal vasculature to hyperoxia and reduced pathological angiogenesis following ischemia in a mouse model of proliferative retinopathy (19). Remarkably, Cyr61/CCN1 also induced adhesion, migration, and differentiation of hematopoietic stem cells into endothelial progenitors and intravitreal injection of hematopoietic stem cells engineered to express Cyr61/CCN1-blocked ischemia-induced neovessel growth subsequent to hyperoxic injury. Conversely, CTGF/CCN2 had no effect on endothelial progenitor growth and differentiation processes, and the functional significance CTGF/CCN2 signaling in disorders of the retinal vasculature has not completely been elucidated.

CTGF/CCN2 is widely expressed during development and in adult tissue, especially in endothelial cells throughout the embryo and in the developing cardiovascular, skeletal, renal, and neuronal systems (20, 21). Studies of diseased tissues from human clinical specimens and animal models established an association between high levels of the CTGF/CCN2 protein and excessive accumulation and deposition of ECM proteins in fibrotic tissues suggesting a pathogenic role for CTGF/CCN2 in fibroproliferative disorders (22). Genetic modification of CTGF/CCN2 gene expression in mice provided some preliminary but controversial information on the role of CTGF/CCN2 during tissue development and diseases. The traditional knockout of CTGF/CCN2 resulted in perinatal lethality due to skeletal deformity, a phenotype similarly observed in knock-out

mice for constitutively expressed ECM proteins, such as the collagens and proteoglycans, suggesting a possible regulatory relationship between CTGF/CCN2 and other ECM proteins (23, 24). However, transgenic models of CTGF/CCN2 overproduction in various tissues exhibited various phenotypes, including no fibrotic reaction, mild fibrosis, and clear fibrotic phenotypes depending on the CTGF/CCN2 levels (25). Other studies have shown that, unlike many ECM proteins, CTGF/CCN2 is not important in developmental angiogenesis, but it is highly pro-angiogenic when administered exogenously in the cornea or other tissues (26–28). In diabetic CTGF hemizygous mice, basal lamina thickening of retinal capillaries was reduced compared with diabetic wild type mice (29). Taken together, these observations suggest that thresholds of CTGF/CCN2 levels are required to induce cell type-specific effects. The requirement of multiple receptors for certain CTGF/CCN2 actions that are not achieved through a single receptor may account for the dose-dependent and contextual effects of this molecule.

Meanwhile, the CTGF/CCN2 protein is structurally organized into the following four distinct domains: (i) insulin-like growth factor-binding protein (IGFBP); (ii) von Willebrand factor type-C repeat; (iii) thrombospondin type-1 (TSP1); and (iv) C-terminal (CT) (30). Increased levels of truncated variants of CTGF/CCN2 containing the IGFBP and von Willebrand factor type-C domains only were found in the vitreous of patients with active proliferative diabetic retinopathy, suggesting that it plays a pathogenic role or represents a surrogate marker of CTGF/CCN2 activity in the disorder (31). Fragments of CTGF/CCN2 have been shown to accumulate in tissue culture or body fluids, and these fragments may retain biological activity distinct from the intact protein (32). Deletion of the CT domain of CTGF/CCN2 generates a dominant negative variant that antagonizes the activity of the native CTGF/CCN2 molecule (33). Thus, the multimodular organization of the CTGF/CCN2 protein is a means of generating through proteolytic cleavage, variants/bioactive domains that exhibit a diverse range of activities and perhaps bioavailabilities in different milieux.

This study uses loss- and gain-of-function approaches to study the role of CTGF/CCN2 in retinal vessel development and repair. A greater emphasis is placed on CTGF/CCN2-mediated retinal vessel remodeling following hyperoxic injury in a mouse model of ischemic retinopathy.

## EXPERIMENTAL PROCEDURES

*Generation of the Adenoviral and Lentiviral Vectors*—Adenovirus encoding p53 mutant was from Vector Biolabs (Philadelphia, PA). Mouse DNAs for full-length CTGF/CCN2, antisense oligonucleotide, AS-CTGF, and mutant variant CTGF- $\Delta$ CT were obtained by PCR amplification using a DNA template obtained from ATCC (Manassas, VA) and cloned into a shuttle vector. The recombinant adenoviruses were produced by co-transfecting an adenoviral shuttle vector with a viral backbone in which the recombinant DNA is driven by the cytomegalovirus promoter. The adenovirus-encoding luciferase protein, Ad-luc, was used as a control for infection. All adenoviruses were replication-deficient and used at 20 multiplicities of infection to infect rat retinal endothelial cells. The lentiviral vectors Inv-CTGF, Inv-AS-CTGF, Inv-CTGF- $\Delta$ CT, Inv-GFP,

<sup>2</sup> The abbreviations used are: ECM, extracellular matrix; CTGF, connective tissue growth factor; OIR, oxygen-induced retinopathy; MMP-2, matrix metalloproteinase-2; IGFBP, insulin-like growth factor-binding protein; CT, C-terminal; qPCR, quantitative PCR; AS, antisense; APMA, aminophenylmercuric acetate.

## CTGF/CCN2 Function in Ischemic Retinopathy

and Inv-luc were produced by transient  $\text{CaPO}_4$ -mediated transfection of 293T cells with lentiviral backbone plasmids, a vesicular stomatitis virus-g-envelope plasmid, and a group antigen/polymerase plasmid. Titers of  $5 \times 10^6$  IU/ml were achieved and concentrated by ultracentrifugation to  $1.5 \times 10^{12}$ – $10^{13}$  IU/ml. Production of lentiviral vectors was performed under the auspices of the National Institutes of Health, NHLBI, Gene Therapy Resource Program Vector Core Laboratory at the University of Pennsylvania.

**Mouse Model of Oxygen-induced Retinopathy (OIR)**—Oxygen-induced retinopathy was produced in C57BL/6J mice as described by Smith *et al.* (34). Neonatal mice and their nursing dams were exposed to 75% oxygen in a PRO-OX 110 chamber oxygen controller from Biospherix Ltd. (Redfield, NY) between postnatal day 7 (P7) and P12. The oxygen flow was monitored and maintained at 75% + 3% of oxygen. On P12, the pups were placed under normoxic conditions until P17 when they were sacrificed, and the retinas were dissected and assessed for maximum neovascular response. For developmental studies, room air mouse pups were raised under normal light and temperature conditions and sacrificed at the indicated time periods after birth by  $\text{CO}_2$  euthanasia and cervical dislocation. The mice were exposed to a 12-h cyclical broad spectrum light. For lentivirus-mediated gene transfer studies, animals were anesthetized by intraperitoneal injection of ketamine (65 mg/kg) and xylazine (35 mg/kg), and a recombinant viral vector ( $\sim 1 \mu\text{l}$ ) was injected into the vitreous in one eye of each animal just below the ora serrata using a 33-gauge needle syringe (Hamilton, Bonaduz, Switzerland). Control vector was injected in the other eye. Eyes were then enucleated, and retinas were dissected and processed for histological and molecular analyses.

**Immunohistochemistry of the Retinal Vasculature**—Enucleated eyes were fixed in 4% paraformaldehyde for 30 min, and retinas were dissected and laid flat on SuperFrost® Plus-coated slides to obtain whole mount preparations. Retinas were flat-mounted through four incisions dividing each into four quadrants and incubated overnight in 10  $\mu\text{g}/\text{ml}$  rhodamine-labeled Ulex Europaeus agglutinin-1 (UEA-1, Vector Laboratories, Burlingame, CA), which binds specifically to the endothelium. Retinas were washed extensively and mounted with 4',6-diamidino-2-phenylindole (DAPI, Vector Laboratories) with the ganglion cell layer uppermost using a coverslip. Images were acquired using an Olympus-BHS microscope attached to a QImaging Retiga 4000RV digital camera. Images were captured with ImagePro Plus (version 5.1) software. The areas of vascular obliteration were measured by delineating the avascular zone in the central retina and calculating the total area using Photoshop CS5 (Adobe). Similarly, the areas of pre-retinal neovascularization were calculated by selecting regions containing tufts, which appear more brightly stained than normal vasculature, based on pixel intensities. Selected regions were then summed to generate a total area of neovascularization. The avascular and neovascular areas were expressed as a percentage of the total retinal area.

**Western Immunoblotting and Fluorescence Microscopy**—For protein analyses, mouse eyes were enucleated, and retinas were carefully dissected and homogenized in lysis buffer containing 10 mM NaF, 300 mM NaCl, 50 mM Tris, pH 7.4, 1% Triton

X-100, 10% glycerol, and 1 mM EDTA with 1% volume of phosphatase and protease inhibitor mixture. Protein samples (50  $\mu\text{g}$ ) were fractionated in a 10% SDS-polyacrylamide gel and transferred to nitrocellulose membrane, and Western blot analysis was performed with antibodies against either CTGF/CCN2 (Aviva Systems Biology, San Diego), MMP-2 (Millipore, Billerica, MA), p53 (Santa Cruz Biotechnology), type IV collagen (Millipore), or GAPDH (Biovision Inc., Mountain View, CA). Immunodetection was performed using enhanced chemiluminescence (ECL) from Pierce. Protein bands were quantified by densitometric scanning. To analyze proteins from cell cultures, cells were homogenized in lysis buffer, fractionated by electrophoresis, and analyzed as described above.

For immunohistochemical analyses, enucleated and paraformaldehyde-fixed eyes were incubated overnight in sucrose solution. A set of eyes was frozen in Tissue-Tek Optimal Cutting Temperature compound, and 12- $\mu\text{m}$ -thick cryostat sections were prepared. Retinas were dissected from another set of eyes and flat-mounted on a glass slide. Cross-sections and flat-mount preparations of retinas were then permeabilized in 0.1% Triton X-100 at room temperature for 20 min. Nonspecific protein binding was blocked by treatment with normal goat serum for 30 min at room temperature. After the blocking step, the preparations were treated for 2 h with either polyclonal rabbit anti-glial fibrillary acidic protein (Invitrogen), polyclonal rabbit anti-CTGF/CCN2 (Aviva Systems Biology), monoclonal anti-rabbit anti-macrophage F4/80 antibody (AbD Serotec, Raleigh, NC), or antibody diluent alone. Immunodetection was performed with either rhodamine- or fluorescein-conjugated anti-rabbit IgG (Vector Laboratories). Retina mounts and sections were washed several times in PBS between incubations. Retinas were imaged with an Olympus Fluorescence microscope via a  $\times 40$  lens.

**Quantitative Real Time PCR (qPCR)**—Steady state levels of specific mRNAs were determined by qPCR using TaqMan technology on an ABI 7000 sequence detection system from Applied Biosystems (Carlsbad, CA). Highly specific primers were designed using Web-based primer design programs. Primers used included the following: 5' GCTTTATCACCTGCACAGCA 3' and 5' GTAACCGGGGAGGGAAATTA 3' for CTGF/CCN2; 5' CGCCATCATCAAGTCC 3' and 5' TTTCAGCACAAAGAGGTTGC 3' for MMP-2; 5' TCTGCTCTCCTTCTGTCGTG 3' and 5' CTCTCTTGGGTGCACAGGA 3' for VEGF; 5' AGGGTCTGGGCCATAGAACT 3' and 5' TCTACTGAACTTCGGGGTGA 3' for TNF- $\alpha$ ; and 5' GCTGAAAGCTCTCCACCTCA 3' and 5' AGGCCACAGGTATTTTGTGCG 3' for IL-1 $\beta$ . The cycling parameters for qPCR amplification reactions were as follows: AmpliTaq activation at 95 °C for 10 min, denaturation at 95 °C for 15 s, and annealing/extension at 60 °C for 1 min (40 cycles). Triplicate *Ct* values were analyzed with Microsoft Excel using the comparative *Ct* ( $\Delta\Delta C_t$ ) method as described by the manufacturer (Applied Biosystems). The transcript amount ( $-2^{\Delta\Delta C_t}$ ) was obtained by normalizing to an endogenous reference (18 S rRNA) relative to a calibrator.

**MMP-2 Activity Assays**—In-gel zymography and Biotrak activity enzyme-linked immunosorbent assays (ELISA) were used to analyze and quantify MMP-2 activity, respectively. Fol-



lowing treatment, mice were sacrificed at P12 and P17, and two retinas were pooled to obtain a sufficient amount of material for analysis. Retinas were homogenized in 50 mM Tris-HCl buffer, pH 7.4, containing 1 mM monothio glycerol. Samples were then centrifuged at  $2000 \times g$  for 10 min at 4 °C. Protein concentration of the soluble fractions was determined using the BCA protein assay kit (Pierce). For in-gel zymography, 20  $\mu$ g of proteins from retinal homogenates were mixed with loading buffer without denaturation agents and assayed for MMP activity by gel zymography using gelatin-containing pre-cast gels from Invitrogen according to the manufacturer's instructions. After electrophoresis, gels were incubated in zymogram renaturation buffer for 1 h, followed by incubation in development buffer at 37 °C for 48 h. Subsequently, gels were stained with 0.1% Coomassie Blue R-250 containing 30% methanol and 10% acetic acid. Destaining was performed in a solution containing 50% methanol and 10% acetic acid. Molecular weights were estimated using prestained molecular weight markers.

MMP-2 Biotrack<sup>TM</sup> activity ELISA (GE Healthcare) was used to accurately measure both endogenously active MMP-2 and total MMP-2 following activation of latent MMP-2 by aminophenylmercuric acetate (APMA). Briefly, MMP-2 standard samples and protein samples (appropriately diluted) from retinal homogenates were added to ELISA plates precoated with MMP-2 antibodies and incubated for 20 h at 4 °C. Chromogenic substrate was added, and color development was recorded in a microplate spectrophotometer at 405 nm at different time intervals (up to 3 h). The amount of total MMP-2 activity (already active plus activatable pro-MMP-2) was measured by incubation of the captured MMP-2 with 0.5 mM APMA for 3 h at 37 °C before addition of chromogenic substrate. Calculation of the relative amounts of MMP-2 in the protein homogenates was made by comparison with the respective standard curves.

**Cell Culture and Transient Transfection with MMP-2 Promoter Vectors**—Retinal endothelial cells were obtained from Cellpro (San Pedro, CA) and maintained in culture according to the manufacturer's instructions. Cells showed positive immunostaining for endothelial cell markers (e.g. CD31) obtained from Miltenyi Biotec (Bergisch Gladbach, Germany). Cells were propagated in 35-mm dishes in predefined endothelial growth medium containing 10% of fetal bovine serum (FBS) from Atlanta Biological Inc. (San Diego). Cells at 80% confluence were treated as described in the text and further processed for various analyses. For cell infection, cells at 80% confluence were first incubated with adenoviral vectors in serum-free medium for up to 3 h and then in serum-containing medium for 16 h. Transfection with plasmids was further performed using FuGENE 6 transfection reagent in serum-free medium according to the manufacturer's specifications (Roche Diagnostics). A 1668-bp DNA fragment of the wild type *MMP-2* promoter, and a series of deletion constructs of this promoter, each ligated to firefly luciferase reporter plasmid were used in transfection experiments (35). Further fine mapping of enhancer activity was performed by preparing a promoter/reporter construct containing a mutated p53-binding element using the Quik-Change site-directed mutagenesis kit (Stratagene, La Jolla, CA). The p53-binding site was changed from 5' CGAAATTGTTTC-

TATAGCCTGCTGGGCAAGTCTGAAATTGTCAGAAAC-CCACTAGACTCAAG 3' to 5' CGAAATTGTTCTATAGCCTGCTGGGTCTATCTGAAATTGTCAGAAACCCACTAGACTCAAG 3'. These nucleotide substitutions abolished the p53-binding site. Construct was fully sequenced in both directions to confirm successful mutagenesis before use. Other co-expression vectors used include the pA-Fos, DN-Egr-, and Admut-p53. Cells were co-transfected with pRL-SV40 vector containing the *Renilla* luciferase gene to adjust for transfection efficiency. The FuGENE 6/DNA mixture plus serum-free medium was left on cells for 3 h. The cells were allowed to recover in fresh medium containing 10% serum. The next day, cells were incubated in serum-free medium for 16 h. Cell lysates were prepared and assayed for luciferase activity levels, and firefly luciferase activity was normalized to that of *Renilla* luciferase. Each experiment was performed at least three times in triplicate, and all experiments included negative (promoterless pGL3-basic) control. The latter served as a base-line indicator of luciferase activity.

**Chromatin Immunoprecipitation (ChIP) Assay**—ChIP was performed as described previously with modifications allowing for a quantitative analysis of protein-DNA interaction (9). DNA-protein complexes were fixed by directly adding formaldehyde (1%) to freshly dissected retinas or cultured cells. Fixation proceeded at 22 °C for 10 min and was stopped by the addition of glycine to a final concentration of 0.125 M. Retinas were then homogenized in lysis buffer (10 mM potassium acetate, 15 mM magnesium acetate, 0.1 M Tris, pH 7.6) containing a mixture of protease inhibitors. The nuclei were collected by microcentrifugation, then resuspended in sonication buffer (1% SDS, 10 mM EDTA, 50 mM Tris-HC, pH 8.1, 0.5 mM phenylmethylsulfonyl fluoride, and 100 ng of leupeptin and aprotinin/ml), and incubated on ice for 10 min. Prior to sonication, 0.1 g of glass beads was added to each sample. The chromatin solution was pre-cleared by centrifugation and incubated with 1  $\mu$ g of affinity-purified rabbit polyclonal antibody or no antibody and rotated at 4 °C for ~12–16 h. Antibodies against p53 were added, and incubation was continued for 24 h. Immunoprecipitation, washing, and elution of immune complexes was carried out. Prior to the first wash, 20% of the supernatant from the reaction with no primary antibody was saved as total input chromatin and was processed with the eluted immunoprecipitates beginning at the cross-link reversal step. Cross-links were reversed by the addition of NaCl to a final concentration of 200 mM, and RNA was removed by the addition of 10  $\mu$ g of RNase A per sample followed by incubation at 65 °C for 4–5 h. The samples were then precipitated at –20 °C overnight with ethanol and then pelleted by microcentrifugation. Samples were treated with proteinase K for 2 h at 45 °C. The pellets were collected by microcentrifugation and resuspended in 30  $\mu$ l of H<sub>2</sub>O. Real time PCR was performed on 1 ng of genomic DNA from ChIP experiments. Two pairs of real time PCR primers were designed to flank the p53-binding element of the *MMP-2* promoter region. Primers used in the final PCR amplification of the *MMP-2* promoter region encompassing the p53-binding site are 5' TGGTCCCAAAGACTCCTTG 3' and 5' TGCCTGACAGAGTTGGAGA 3'; alternatively, PCR products were

## CTGF/CCN2 Function in Ischemic Retinopathy

fractionated by electrophoresis on 2% agarose gel and quantified by scanning densitometry.

**Statistical Analysis**—Data were expressed as means  $\pm$  S.E. To test differences among several means for significance, a one-way analysis of variance with the Newman-Keuls multiple comparison test was used. Where appropriate, post hoc unpaired *t* test was used to compare two means/groups, and *p* values  $<0.05$  or  $<0.01$  were considered significant. Statistical analyses were performed using the Prism software for Windows version 4 (GraphPad Inc, San Diego).

### RESULTS

**Regulation of CTGF/CCN2 Gene Expression in the Retinal Vasculature during Development and in Response to Hyperoxia**—Development of mouse retinal vessels, which occurs during the first 3 weeks after birth, is characterized by an initial radial growth from the optic disc followed by the development of intraretinal capillaries. Therefore, we examined whether this active angiogenic process involves changes in the expression pattern and/or localization of CTGF/CCN2 in the developing mouse retinal vasculature. As shown in Fig. 1A, CTGF/CCN2 mRNA levels increased steadily and progressively between P2 and P6 as superficial retinal vessels expand to cover the surface of the retina and continued increasing progressively at P12 to P14 after a transient decrease at P10 when the secondary deep layer of the retinal vasculature starts extending and growing radially outward toward the inner nuclear and outer plexiform layers. The CTGF/CCN2 mRNA levels then progressively declined but maintained relatively high basal expression levels as the adult vasculature was established. Immunoreactivity to the CTGF/CCN2 protein at P12 was observed in superficial retinal vessels, which grow radially from the optic nerve, and in the deeper retinal vasculature that forms during the 2nd week through branching of the superficial layer (Fig. 1B). In cross-sectioned retinas, astrocytes, retinal pigment epithelial cells, and some cells in the inner nuclear layer showed positive immunoreactivity to the CTGF/CCN2 protein (data not shown), which accounts for the relatively high background immunostaining around retinal vessel in flat-mounted retinas.

The expression pattern of CTGF/CCN2 was then examined in the mouse model of OIR. As shown in Fig. 1C, the steady state mRNA levels of CTGF increased 3.8 times as retinal vessels develop and mature between P12 and P17 confirming previously reported observations by Pi *et al.* (36). The retinopathy response characterized by neovessel growth was associated with a 6.4-fold increase of CTGF/CCN2 mRNA levels that were 3.5 times higher than their levels under normoxic conditions at P17 (Fig. 1C). At this stage, a strong immunoreactivity to CTGF/CCN2 protein was observed in neovascular tufts, which protrude luminally in the vitreous (Fig. 1D).

**Effect of CTGF/CCN2 Overexpression on Hyperoxia-induced Retinal Vessel Obliteration and Neovessel Formation**—Given the dynamic changes of CTGF/CCN2 gene expression during normal and abnormal retinal vessel formation, we examined the impact of gain- and loss-of-function of CTGF/CCN2 during development and following OIR. Lentiviral vectors were used because of their transgene capacity, rapid onset of expression, and robust and sustained gene expression profile (37). Intravit-

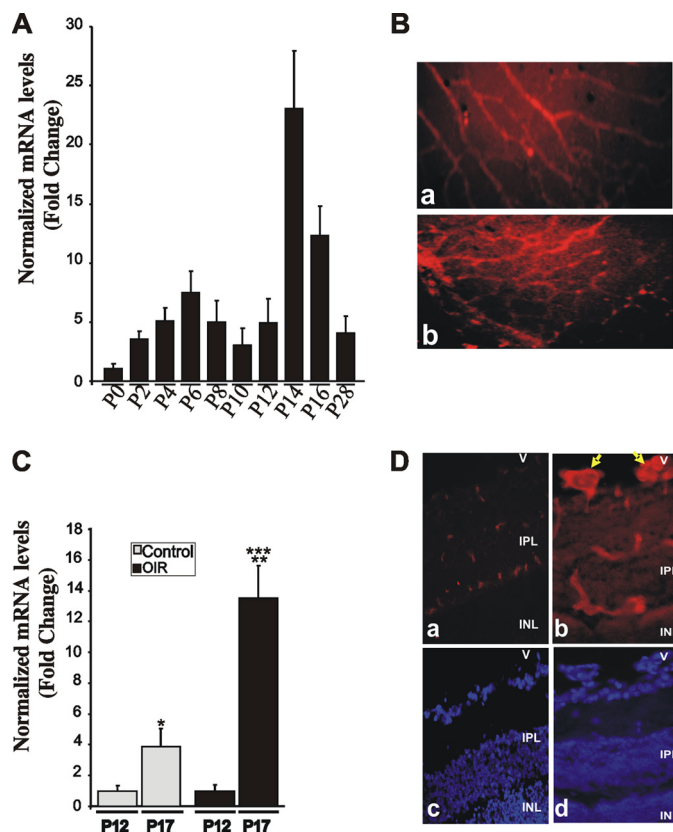


**FIGURE 1. Expression and tissue localization of CTGF/CCN2 during normal retinal vessel development and in response to OIR.** A, room air mouse pups were raised under normal light and temperature conditions, sacrificed at the indicated time periods, and retinas dissected. CTGF/CCN2 mRNA levels were quantified by qPCR and normalized to those of 18 S rRNA. The  $\Delta\Delta Ct$  values are the average of determinations from tissue samples obtained from 4 to 9 animals each measured in triplicate. B, immunohistochemical localization of the CTGF/CCN2 protein in flat-mount preparations of retinas at P12. All retinal preparations were fixed in 4% paraformaldehyde and permeabilized prior to immunostaining with anti-CTGF/CCN2 antibody. Immunoreactivity to CTGF/CCN2 in the superficial and deeper retinal vessels is shown in panels a and b, respectively. Magnification,  $\times 40$ . C, expression pattern of CTGF/CCN2 mRNA following the hyperoxic (P7 to P12) and ischemic (P12 to P17) phases of OIR as determined by qPCR. CTGF/CCN2 mRNA levels were normalized to those of 18 S rRNA. Data are means  $\pm$  S.E. ( $n = 4$  animals). \*,  $p < 0.05$  versus P12/Control. \*\*,  $p < 0.001$  versus P12/OIR. \*\*\*,  $p < 0.05$  versus P17/Control. D, immunolocalization of CTGF/CCN2 (panels a and b) in 10- $\mu$ m-thick cross-sections of retinas from P17 control (panel a) and OIR (panel b) retinas. Nuclear staining with DAPI of cross-sections (panels a and b) is shown in panels c and d, respectively. Arrows indicate CTGF/CCN2 immunostaining in neovascular tufts protruding luminally in the vitreous. V, vitreous; IPL, inner plexiform layer; INL, inner nuclear layer. Magnification,  $\times 40$ .

real injection of a lentivirus expressing the GFP gene (Inv-GFP) prior to OIR showed a widespread localization and distribution of GFP fluorescence throughout the retinal layers (supplemental Fig. S1A). In cross-sectioned retinas, GFP fluorescence was detected in an irregular distribution across the neural retina, which is consistent with the neurotropic effects of lentiviral vectors. Such a property was attributed to the envelope glycoprotein derived from vesicular stomatitis virus-g (38). The proportion of retinal cells transduced by Inv-GFP in a series of random sections (6–12 sections) that spanned at least 50% of the retinal surface varied between 45 and 79%. Retinal pigment epithelium exhibited fluorescence as well, although this was undistinguishable from the inherent autofluorescence of this layer (data not shown). In flat-mounted preparations of retinas,



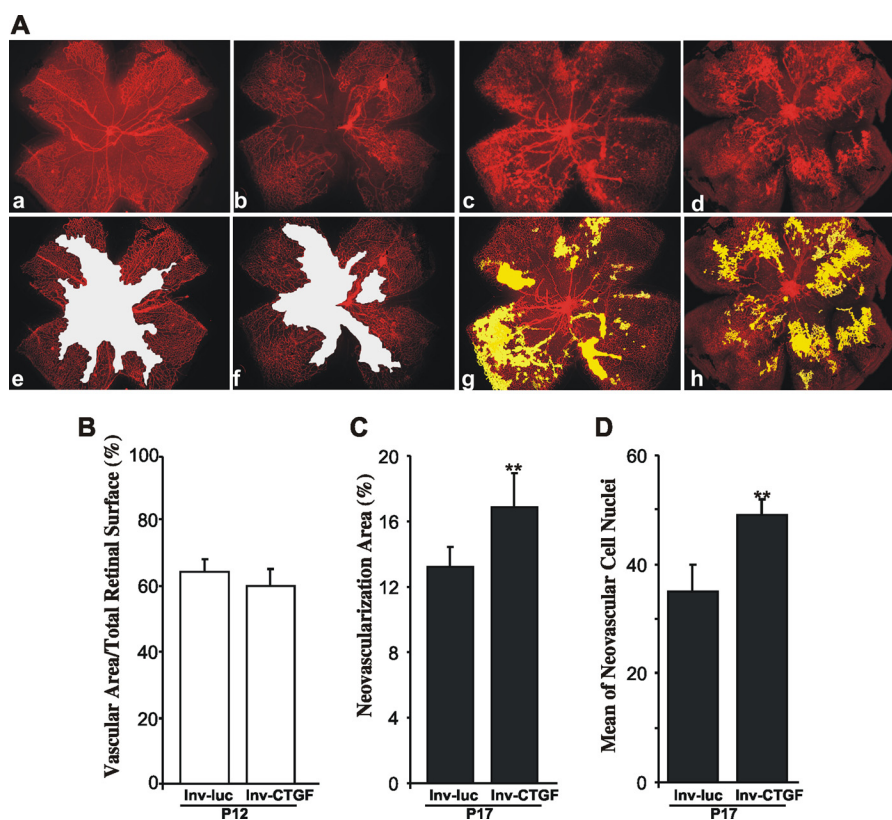


**FIGURE 2. Effects of lentivirus-mediated expression of CTGF/CCN2 on vaso-obliteration and retinal neovascularization following OIR.** A, representative flat-mount preparations of rhodamine-UEA-1-stained retinas from OIR eyes at P12 (panels a and b) and P17 (panels c and d) injected with either Inv-luc (panels a and c) or Inv-CTGF (panels b and d). Areas of vaso-obliteration and pre-retinal neovascular tufts as determined by computer-assisted image analyses are shown in white (panels e and f) and yellow (panels g and h), respectively (panel e for panel a; panel f for panel b; panel g for panel c; and panel h for panel d). Magnification,  $\times 4$ . B and C, compiled data showing percentage of vascularized and neovascular tuft areas in Inv-luc- and Inv-CTGF-injected eyes. \*\*,  $p < 0.05$  versus Inv-luc. ( $n = 6-8$ ). D, extent of neovascularization as determined by count of number of nuclei in random mid-peripheral areas of retinas. \*\*,  $p < 0.05$  versus Inv-luc, ( $n = 4$ ).

GFP fluorescence can be observed in vascular cells, including those that are not embedded within the basement membrane, possibly pericytes and astrocytes (supplemental Fig. S1B). Furthermore, the extent of the areas of vaso-obliteration at P12 and neovascularization at P17 was similar in noninjected OIR eyes and those injected with a control lentiviral vector (e.g. Inv-luc, Inv-GFP) (data not shown), suggesting that lentiviral vector injection alone had no significant impact on the retinopathy response.

First, we determined whether ectopic expression of the *CTGF/CCN2* gene through intravitreal injection at P4 of the recombinant viral vector, Inv-CTGF, modulates neovascularization following OIR. Examination of flat-mounted retinas demonstrated several similarities and some fundamental differences between Inv-CTGF- and control Inv-luc-injected eyes. At P12, vaso-obliteration in the retinas from Inv-luc- and Inv-CTGF-injected eyes was clearly evident, and the extent of vaso-obliterated areas was nearly identical in both groups of eyes (Fig. 2, A and B). However, at P17, retinal neovascular tufts, which can be seen in the central and mid-peripheral retina in Inv-luc-injected eyes, were more abundantly present in eyes injected with the Inv-CTGF vector, and in many cases they extended to the peripheral retinal areas. Quantification of pre-retinal neovascularization at P17 (when maximum pre-retinal neovascularization occurs) showed a 25% increase of neovascular tuft areas in Inv-CTGF-injected eyes as compared with Inv-

luc-injected ones (Fig. 2C). Similarly, the score of neovascular cell nuclei defined as the mean number of neovascular cell nuclei per retinal cross-section on each side of the optic nerve was significantly higher ( $p < 0.05$ ) in Inv-CTGF-injected eyes versus Inv-luc-injected eyes (Fig. 2D). Clearly, ectopic overexpression of *CTGF/CCN2* further exacerbated and accelerated retinal neovascularization in response to ischemia.

Next, we examined the distribution pattern of astrocytes and macrophages. These cells have the potential to release cytokines, regulate neovascular tuft formation, and dictate whether endothelial cells proliferate, migrate, and incorporate into pathological vessels or undergo apoptosis (39). Overexpression of *CTGF/CCN2* increased the number of active glial fibrillary acidic protein-positive microglial cells that spread and adopt an amoeboid form, in contrast to nonactive microglial cells that adopt a filiform quiescent shape (Fig. 3A). However, there was no alteration in the total number of astrocytes between Inv-luc and Inv-CTGF-injected eyes (data not shown). The number of F4/80 antigen-positive macrophages was significantly increased at P17 in Inv-luc- and Inv-CTGF-injected eyes as compared with their levels at P12, but no significant change was seen between these two groups at P17 (Fig. 3B).

To examine the underlying molecular effectors of the neovascular response to *CTGF/CCN2* overexpression, we determined the transcript abundance of key genes commonly asso-

## CTGF/CCN2 Function in Ischemic Retinopathy

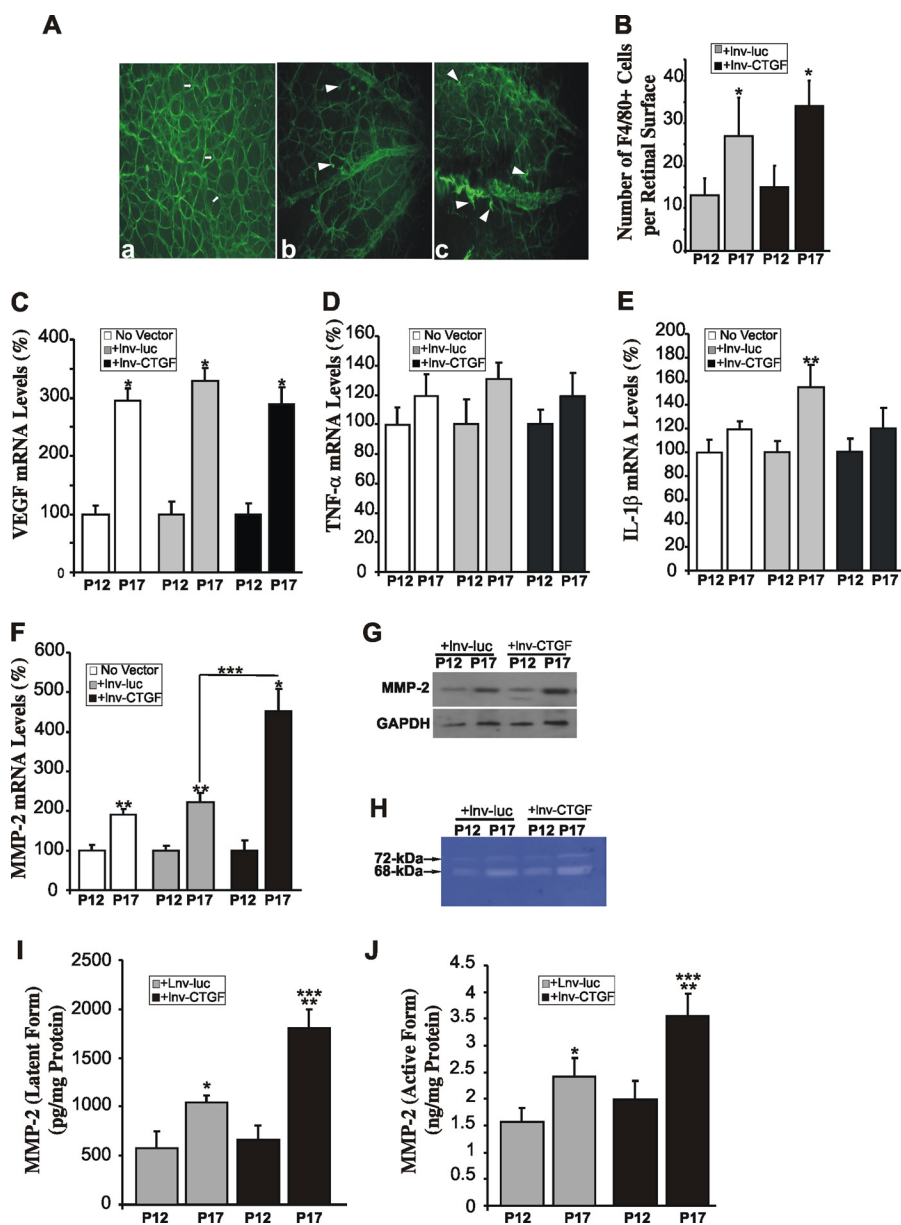


**FIGURE 3. Modulation of inflammatory and angiogenic factors in response to CTGF/CCN2 overexpression in OIR mice.** *A*, alteration in microglia phenotype in ischemic areas of OIR retinas at P17. Microglial cells, which include astrocytes, were visualized in flat-mounted retinas from mice following either normoxia (*panel a*) or OIR with injection of Inv-luc (*panel b*) or Inv-CTGF (*panel c*). Note the predominance of cells with extensive ramifications (shown with arrows in *panel a*) and their scarcity and appearance of amoeboid-shaped cells (shown by arrowheads in *panels b* and *c*). *B*, enumeration of F4/80+ macrophages in flat-mounted OIR retinas following injection of Inv-luc or Inv-CTGF. Vector injection was performed at P4, and macrophage detection was performed using F4/80 antibody. Macrophage count was performed separately in each quadrant of retina and normalized to the retinal surface to facilitate comparisons among different animals. \*,  $p < 0.05$  ( $n = 5$ ). *C–F*, steady state mRNA levels of VEGF, TNF- $\alpha$ , IL-1 $\beta$ , and MMP-2 as determined by qPCR in retinas from noninjected OIR eyes as well as those injected with either Inv-luc or Inv-CTGF. The data shown are the means  $\pm$  S.E. of three determinations each performed in triplicate. RNA levels at P12 were set to 100% to facilitate comparison among experiments and groups. \*,  $p < 0.01$  versus P12 ( $n = 7$ ). \*\*,  $p < 0.05$  versus P12 ( $n = 7$ ). \*\*\*,  $p < 0.05$  versus P17/Inv-luc ( $n = 7$ ). *G*, Western blot analysis of the MMP-2 protein in retinal tissue lysates from OIR mice injected with either Inv-luc or Inv-CTGF. GAPDH was used as protein loading control. *H*, in-gel zymography of MMP-2 in retinal tissue homogenates from OIR eyes injected with either Inv-luc or Inv-CTGF lentiviral vectors. Latent and active MMP-2 activities were determined by an immunosorbent-based MMP-2-specific Biotrack assay with and without activation by APMA, respectively, as described under "Experimental Procedures." Amounts of MMP-2 in the samples were determined by interpolation from a standard curve. Values are means  $\pm$  S.E. from three sets of eyes. \*,  $p < 0.01$  versus P12 ( $n = 3$ ). \*\*,  $p < 0.05$  versus P12 ( $n = 3$ ). \*\*\*,  $p < 0.01$  versus P17/Inv-luc ( $n = 3$ ).

ciated with neovascularization, including *VEGF*, *TNF- $\alpha$* , *IL-1 $\beta$* , and *MMP-2*. Ischemia significantly and consistently increased the steady state mRNA levels of the *VEGF* gene in noninjected eyes as well as those injected with either Inv-luc or Inv-CTGF vector (Fig. 3C). The mRNA levels of *TNF- $\alpha$*  were not significantly increased at P17, and those of *IL-1 $\beta$*  were elevated but only significantly in the Inv-luc-injected eyes (Fig. 3, D and E).

These data are consistent with those reported by others, although small discrepancies in the extent of mRNA level changes exist due to the well known variability of the retinopathy response in mice (40, 41). Nevertheless, ischemia-induced retinal neovascularization requires neither *TNF- $\alpha$*  nor *IL-1 $\beta$* , which have been shown to affect mostly leukostasis and vascular leakage in the OIR mouse model (42). The expression of



*COL1A1* and *COL4A1* chains was not significantly altered, whereas that of thrombospondin 1 was increased by 20% only (data not shown). Interestingly, ischemia significantly increased the mRNA levels of MMP-2 at P17, and overexpression of *CTGF/CCN2* resulted in an even greater (>4-fold) increase of *MMP-2* transcript levels as compared with a 2-fold increase in response to control vector overexpression (Fig. 3F). These changes correlated well with an increase of MMP-2 protein levels as determined by Western immunoblotting (Fig. 3G). Gelatin zymography for MMP-2 activity, which is at least 100 times more sensitive than Western blotting, showed a strong active band of ~68 kDa and a lighter band that likely corresponds to the latent 72-kDa form of MMP-2 (Fig. 3H). This pattern of MMP-2 activity in retinal tissue is consistent with that previously reported by others (43). Furthermore, we used the Biotrak MMP-2 activity assay to more accurately measure the levels of endogenously active and latent (following activation by APMA) forms of MMP-2. As shown in Fig. 3, I and J, *CTGF* overexpression significantly increased the levels of both the proenzyme and the corresponding cleaved active form of MMP-2 as compared with overexpression of the control reporter gene in OIR mice. Changes of the proenzyme levels were correlated with those seen at the mRNA levels suggesting that *CTGF/CCN2* overexpression enhanced both *MMP-2* gene transcription and protein translation and activity. Given that CTGF protein abundantly localized in neovascular areas, the associated changes of *MMP-2* expression and activity may be confined to targeted retinal areas, particular vessels, and perhaps specific cells.

**Effects of *CTGF/CCN2* Depletion on Hyperoxia-induced Retinal Vessel Obliteration and Neovessel Formation**—Loss of *CTGF/CCN2* function in the retina was performed through intravitreal injection of two vectors. The first vector, Inv-AS-CTGF, is a lentiviral vector encoding an antisense DNA fragment complementary to the 5' region overlapping the initiation of transcription site of *CTGF/CCN2* and was designed to interfere with *CTGF/CCN2* gene transcription. Analysis of retinal protein homogenates from eyes injected with Inv-AS-CTGF and subjected to OIR showed that this vector reduced CTGF transcript and protein levels by 60% (supplemental Fig. S1, C and D). The second vector, Inv-CTGF- $\Delta$ CT, is a mutant form of the *CTGF/CCN2* protein lacking the C-terminal domain. This mutant variant acts as a dominant negative form of the wild type protein and inhibits *CTGF/CCN2* activity (32, 33). The expression and migratory pattern of CTGF- $\Delta$ CT as compared with the full-length *CTGF/CCN2* protein were confirmed by gel electrophoresis of retinal protein homogenates from eyes injected with either Inv-luc, Inv-CTGF, or Inv-CTGF- $\Delta$ CT (supplemental Fig. S1E).

We first examined the effects of Inv-AS-CTGF and Inv-CTGF- $\Delta$ CT on retinal vessel sprouting and assembly during postnatal development through intravitreal injection of these vectors. As shown in Fig. 4A, the formation of the superficial layer of retinal vessels is normally complete in eyes injected with control Inv-luc vector, reaching the retinal periphery by P7. However, development and maturation of the vasculature were delayed in the retina following injection of either Inv-AS-CTGF or Inv-CTGF- $\Delta$ CT. Inhibition of *CTGF/CCN2* expres-

sion/activity did not inhibit but delayed the spreading of the superficial capillary plexus by ~10–15% of the distance from the optic nerve head to the retinal periphery suggesting that adequate levels of *CTGF/CCN2* are needed for normal retinal vessel migration and patterning.

Next, we examined the retinal vessel phenotype in OIR mice following injection of either Inv-AS-CTGF or Inv-CTGF- $\Delta$ CT. Retinal vessel sensitivity to hyperoxia at P12 was not affected by injection of either Inv-AS-CTGF or Inv-CTGF- $\Delta$ CT as the degree of vaso-oblivation was similar to that of retinas from eyes injected with the control vector (Fig. 4C). Conversely, neovascularization was reduced by 46 and 59% in Inv-AS-CTGF- and Inv-CTGF- $\Delta$ CT-injected eyes, respectively, as compared with control vector-injected eyes (Fig. 4, B and D). Injection of Inv-CTGF- $\Delta$ CT appeared to be more efficient than Inv-AS-CTGF in inhibiting neovessel formation, although differences between the two vectors were not statistically significant.

VEGF transcript levels were reduced at P17 by 18 and 33% in Inv-AS-CTGF- and Inv-CTGF- $\Delta$ CT-injected eyes, respectively (Fig. 4E). In contrast, inhibition of *CTGF/CCN2* had no effect on IL-1 $\beta$  transcript levels (data not shown). *MMP-2* gene transcription was significantly reduced by 40% in either Inv-AS-CTGF- or Inv-CTGF- $\Delta$ CT-injected eyes (Fig. 4F). These changes of *MMP-2* gene transcription correlated well with a simultaneous reduction of the levels of the latent and active forms of MMP-2 in eyes injected with either Inv-AS-CTGF or Inv-CTGF- $\Delta$ CT (Fig. 4, G and H).

***CTGF/CCN2* Activates the *MMP-2* Promoter through a p53-binding Element**—*MMP-2* expression has previously been linked to arterial enlargement that occurs in response to ischemia, and its expression regulates retinal and tumor-induced angiogenesis (44, 45). Its transcriptional requirements are stimulus-dependent and involve cell type-specific trans-acting factors. As shown in Fig. 5A, the *MMP-2* promoter region contains several highly conserved consensus sequences for binding of AP-1, Sp1, AP-2, IRE, and p53 transcription factors. To identify the specific transcriptional requirements for *CTGF/CCN2*-induced *MMP-2* gene expression, cultured retinal endothelial cells were infected with Ad-CTGF and further transfected with either a 1668-bp DNA fragment of the wild type *MMP-2* promoter or a series of deletion constructs of the *MMP-2* promoter, each ligated to firefly luciferase reporter gene (Fig. 5B). Cells infected with Ad-luc vector were used as control. The reporter gene activity was then determined in the cell lysates after cell incubation for 16 h in serum-free medium. All *MMP-2* promoter-reporter constructs exhibited basal activity levels in Ad-luc- and Ad-CTGF-infected cells. However, overexpression of *CTGF/CCN2* resulted in a strong increase (up to 89-fold) of luciferase activity of promoter-reporter constructs retaining at least 1433 bp upstream of the initiation start site of the *MMP-2* gene (Fig. 5B). When the segment length was reduced to 1007 bp, the promoter reporter construct lost more than 65% of its inducibility by *CTGF/CCN2* suggesting that the DNA segment between -1433 and -1007 exhibits the characteristics of an activator/enhancer element. This segment contains a typical p53 cis-acting element that is remarkably conserved in several vertebrate animals, including mouse, rat, and cow (46). A chimeric construct with a p53-mutated sequence reduced the

## CTGF/CCN2 Function in Ischemic Retinopathy

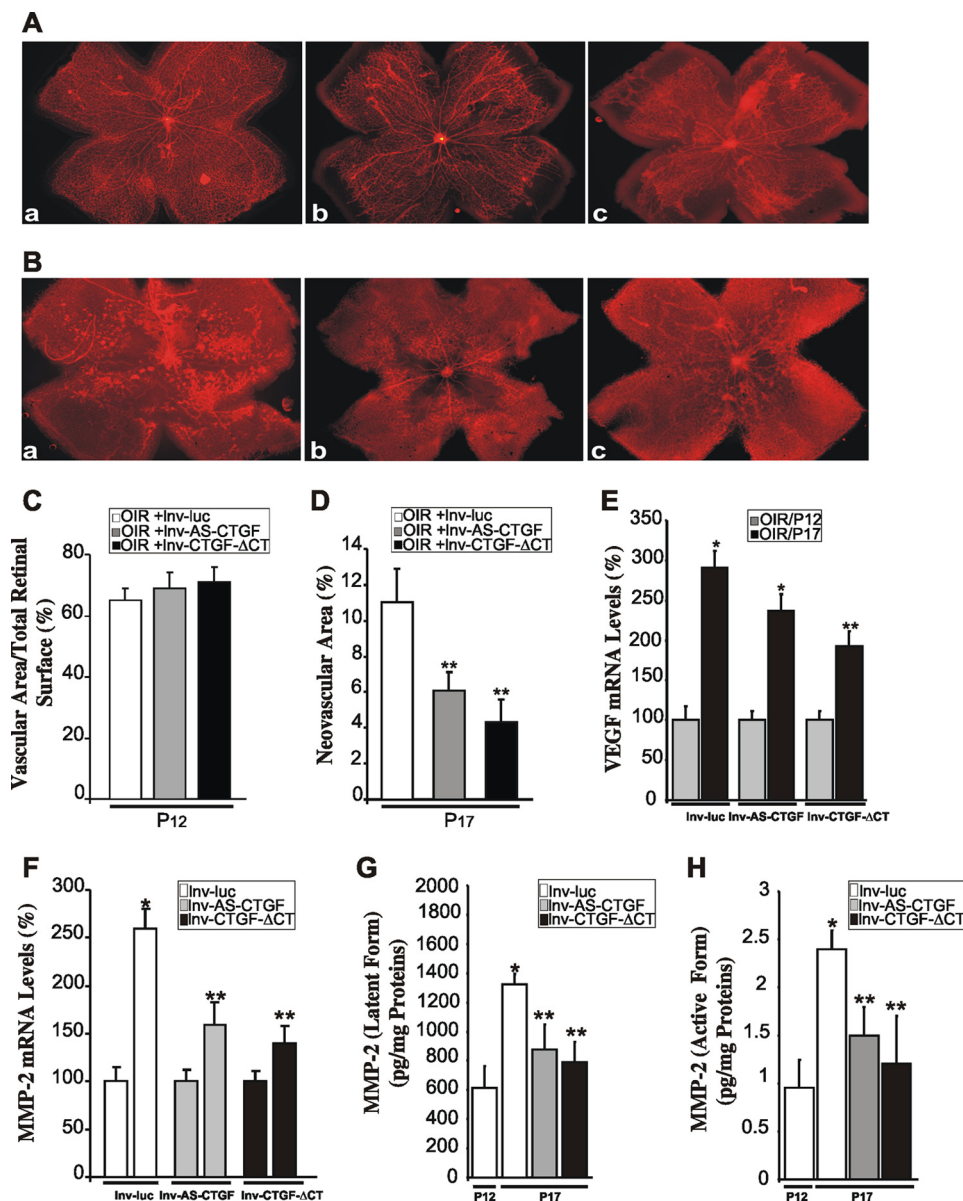


**FIGURE 4. Inhibition of CTGF/CCN2 gene expression or protein activity reduced retinal neovascularization and inhibited MMP-2 gene expression and activity.** A, injection of Inv-AS-CTGF or Inv-CTGF-ΔCT delays blood vessel development and expansion to the retinal edge. Mouse pups were intravitreally injected at P3 with either Inv-luc (panel a), Inv-AS-CTGF (panel b), or Inv-CTGF-ΔCT (panel c) vector. Retinal flat mounts were prepared at P7 and stained with rhodamine-labeled UEA-1. B–D, effects of lentivirus-mediated expression of AS-CTGF and CTGF-ΔCT on retinal neovascularization following OIR. Representative flat-mount preparations of rhodamine-UEA-1-stained retinas from OIR eyes at P17 previously injected with either Inv-luc (panel a), Inv-AS-CTGF (panel b), or Inv-CTGF-ΔCT (panel c) are shown. Areas of vaso-obliteration at P12 and pre-retinal neovascular tufts at P17 were measured by computer-assisted image analyses, and the compiled data showing percentage of avascular and neovascular areas are shown in C and D, respectively. \*\*,  $p < 0.05$  versus OIR/Inv-luc ( $n = 6–8$ ). E and F, transcript levels of VEGF and MMP-2 as determined by qPCR in retinas from OIR mice injected with either Inv-luc, Inv-AS-CTGF, or Inv-CTGF-ΔCT. The data shown are the means  $\pm$  S.E. of three determinations each performed in triplicate. RNA levels at P12 were set to 100% to facilitate comparison among experiments. \*,  $p < 0.01$  versus P12 ( $n = 6$ ). \*\*,  $p < 0.05$  versus either P12 or P17/Inv-luc ( $n = 6$ ). \*\*\*,  $p < 0.05$  versus P17/Inv-luc ( $n = 6$ ). G and H, levels of latent pro-MMP-2 and active MMP-2 in retinal homogenates from OIR eyes injected with either Inv-luc, Inv-AS-CTGF, or Inv-CTGF-ΔCT lentiviral vectors. Latent and active MMP-2 activities were determined using MMP-2-specific Biotrack assay. Amounts of MMP-2 in the samples were determined by interpolation from a standard curve. Values are means  $\pm$  S.E. from three sets of eyes. \*,  $p < 0.01$  versus P12/Inv-luc. \*\*,  $p < 0.05$  versus P17/Inv-luc.

reporter activity by greater than 60% suggesting that the p53 sequence is involved in the *MMP-2* promoter responsiveness to stimulation by CTGF/CCN2. Co-transfection of the cells with Ad-mutp53, which express a dominant mutant of p53, resulted in a 3.3-fold reduction of the reporter activity (Fig. 5C). Interestingly, pA-Fos, a dominant negative form of AP-1, also reduced the reporter activity by 23% suggesting that AP-1 site contributes to CTGF/CCN2-induced *MMP-2* promoter activation. However, co-transfection with Ad-mutp53 and A-Fos

constructs did not result in an additive effect suggesting that p53 is critical for the promoter enhanced activity, although AP-1 may most likely act as a co-activator of the *MMP-2* gene. A dominant negative form of Egr-1 (DN-Egr-1) had no effect on the *MMP-2* promoter activation. Immunoprecipitation of chromatin with p53 antibody showed that p53 interacts with the *MMP-2* promoter within the context of chromatin in Ad-CTGF-transduced cells (Fig. 5D). Conversely, co-transfection of cells with Ad-CTGF and either Ad-AS-CTGF or Ad-CTGF-

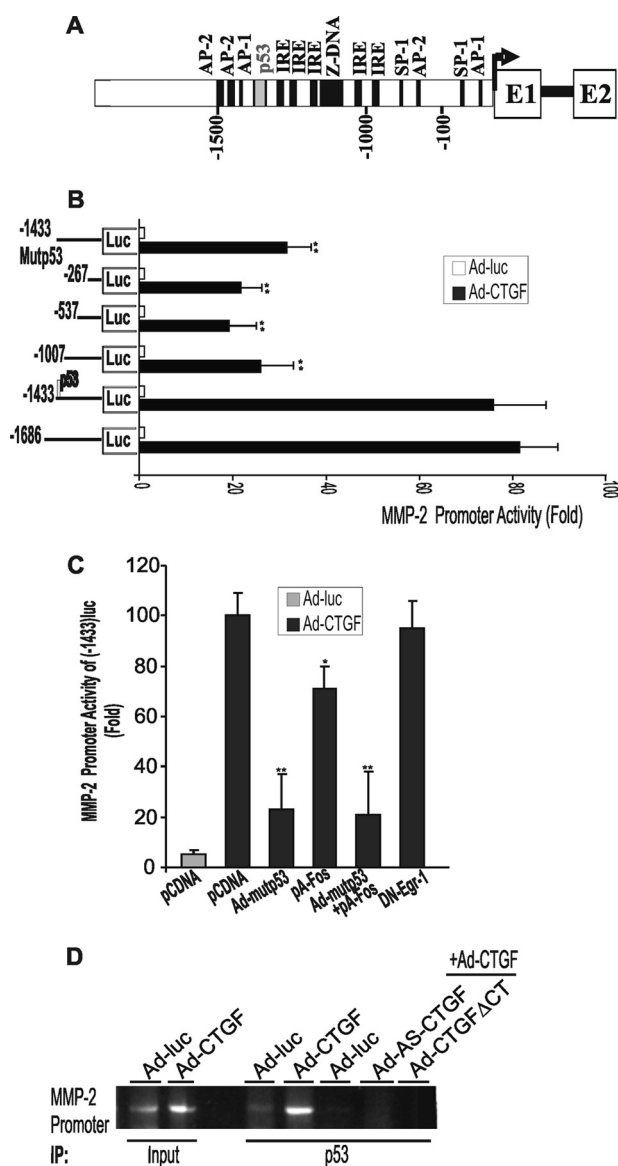


**FIGURE 5. CTGF/CCN2 induces a p53-dependent activation of the *MMP-2* gene.** *A*, schematic representation of the 5' promoter region of the rat *MMP-2* gene containing potential cis-elements for specific transcription factor binding. *B*, p53-binding site in the *MMP-2* promoter is a CTGF/CCN2-responsive element. Retinal ECs were first infected with Ad-CTGF, an adenoviral vector expressing the CTGF/CCN2 gene, and then transiently transfected with each of five *MMP-2* promoter-luciferase (*luc*) reporter constructs shown schematically on the left. Cells infected with Ad-luc under the same conditions were used as controls. Twenty four hours after transfection, cells were incubated in serum-free medium for 16 h. The firefly luciferase activity of the reporter gene was measured in cell lysates and normalized to that of *Renilla* luciferase activity from a co-transfected plasmid as described under "Experimental Procedures." Reporter activity of a construct (-1433-luc) bearing a mutated p53-binding element was tested and shown as well. The graph shows percentage increase in luciferase activity in cells transduced with Ad-CTGF (black bars) over that of control cells transduced with Ad-luc (white bars). Each *MMP-2* promoter reporter construct was assayed in triplicate transfections in at least two independent experiments. The results are expressed as the mean  $\pm$  S.E. \*\*,  $p < 0.01$  versus (-1686) luc construct. *C*, cells transduced with Ad-CTGF were further transfected with the *MMP-2* promoter reporter construct (-1433)luc along with either an empty vector (pCDNA), Ad-mutp53, a mutant variant of p53, pA-Fos, DN-Egr-1, or a combination of A-mutp53 and pA-Fos. Protein lysates were then assayed for luciferase activity following incubation in serum-free medium for 16 h. The relative luciferase activity (mean  $\pm$  S.E.) from a representative transfection experiment performed in triplicate is shown. These experiments were repeated twice using different cell preparations with similar results. \*,  $p < 0.05$  and \*\*,  $p < 0.01$  versus Ad-CTGF (+pCDNA). *D*, p53 enrichment of endogenous *MMP-2* promoter as deter-

$\Delta$ CT prevented interaction of p53 with the endogenous *MMP-2* promoter clearly establishing a critical role of CTGF-induced p53 in the transactivation of the endogenous *MMP-2* gene.

*Anti-CTGF/CCN2 Treatment Reduced Retinal Neovascularization by Decreasing p53 Expression and MMP-2 Activity*—p53 is a tumor suppressor and transcription factor that have been shown to transcriptionally activate the expression of important genes involved in the regulation of cell growth, angiogenesis, and apoptosis (47). Therefore, we examined the *in vivo* relevance of p53 as a molecular effector of CTGF/CCN2-induced *MMP-2* expression in retinal neovascularization. As shown in Fig. 6A, the retinal levels of p53 were significantly increased at P17 both under normoxic and OIR conditions. Injection of Inv-luc control vector did not result in significant changes of p53 levels as compared with noninjected eyes (data not shown). However, ectopic expression of either AS-CTGF or CTGF- $\Delta$ CT prior to OIR significantly reduced p53 levels at P17. Similarly, quantitative ChIP assay showed a 4-fold increase of p53 enrichment of the *MMP-2* promoter region encompassing the p53 binding sequence at P17 (Fig. 6B). However, the levels of this protein-DNA complex were significantly diminished upon ectopic expression of either AS-CTGF or CTGF- $\Delta$ CT prior to OIR, which underscores the importance of p53 in CTGF-mediated regulation of *MMP-2* in OIR retinas. Of note is that CTGF inhibition did not influence *MMP-2* promoter enrichment with p53 following hyperoxia alone (data not shown), suggesting that CTGF-induced *MMP-2* expression minimally affected hyperoxia-induced vaso-obliteration and predominantly influenced neovascularization.

Moreover, intravitreal injection of Pifithrin- $\alpha$ , a selective cell-permeable chemical inhibitor of p53 that inhibits p53-dependent transactivation of p53-responsive genes, significantly reduced neovascular tuft formation at P17 in OIR retinas by nearly 40% as compared with vehicle alone (Fig. 6, C and E). In many cases, neovascular tufts appeared to be reduced/absent in most of the central retinas where they normally form and were confined to a small area of the retina possibly where the Pifithrin- $\alpha$  concentration was the least. Interestingly, more than 50% of Pifithrin- $\alpha$ -injected retinas exhibited a net increase in avascularized surfaces, although the increase did not reach statistical significance (Fig. 6D). However, such a trend suggests that p53 inhibition may cause a widespread suppression of cell growth throughout the retina. Furthermore, Pifithrin- $\alpha$  treatment reduced the expression of the *MMP-2* gene by 50% (Fig. 6F). The binding of p53 in the context of the endogenous *MMP-2* promoter was reduced when nuclear chromatin from Pifithrin- $\alpha$ -injected eyes was subjected to the ChIP assay, which is consistent with reduced transactivation of the *MMP-2* gene upon p53 inhibition.

## DISCUSSION

CTGF/CCN2 is a nonstructural bioactive ECM molecule that bridges the functional divide between structural macro-

mined by ChIP assay. Immunoprecipitated (IP) DNA was detected by PCR and resolved on agarose gel. ChIP assay experiments were repeated twice with different cell preparations with nearly identical results.



## CTGF/CCN2 Function in Ischemic Retinopathy

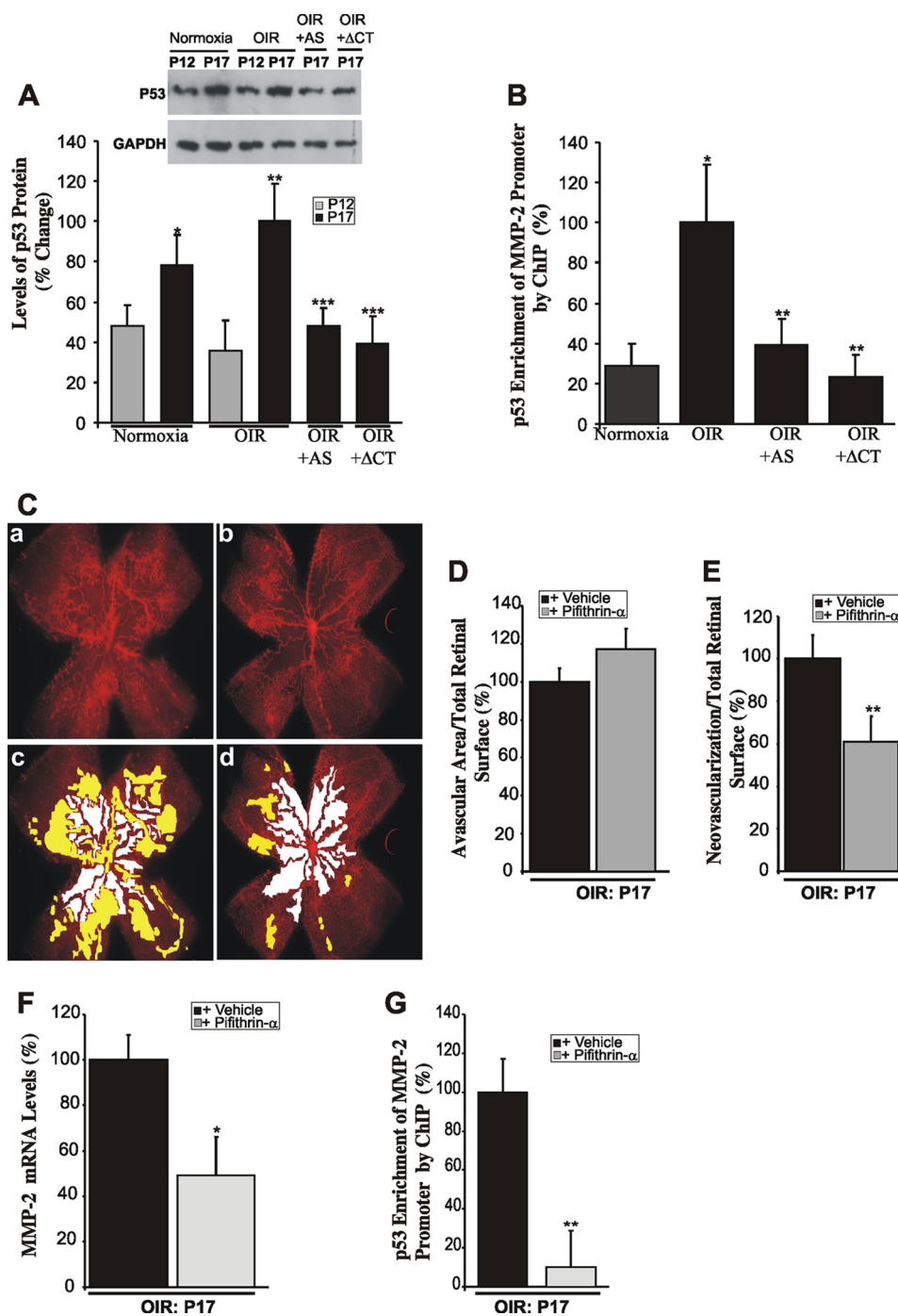


**FIGURE 6. Inhibition of CTGF/CCN2 expression/activity reduced retinal neovascularization by inhibiting p53-dependent transactivation of the MMP-2 gene.** A, Western blot analysis showing the expression pattern of the p53 protein in mouse retinas under normoxia and in OIR mice treated with either Inv-AS-CTGF or Inv-CTGF-ΔCT. Densitometric analysis of the protein band intensity from three independent experiments is shown. \*,  $p < 0.05$  versus P12/normoxia; \*\*,  $p < 0.01$  versus P12/OIR; \*\*\*,  $p < 0.001$  versus P17/OIR. B, p53 enrichment of the endogenous MMP-2 promoter as determined by quantitative ChIP assay in P17 normoxic and OIR retinas with or without ectopic expression of AS-CTGF (+AS) or CTGF-ΔCT (+ΔCT). The p53 enrichment in nonpretreated OIR retinas was set to 100% to facilitate comparisons among different experiments and groups. Data are means  $\pm$  S.E. of three experiments. \*,  $p < 0.001$  versus normoxia; \*\*,  $p < 0.01$  versus OIR. C, representative flat-mount preparations of rhodamine-UEA-1-stained retinas at P17 from OIR eyes previously injected with vehicle (panel a) or Pifithrin- $\alpha$  (panel b). Highlighted avascular (white) and neovascular (yellow) areas are shown in panels c and d. D and E, percentage of avascular and neovascular areas at P17 was measured as described in Fig. 2. \*\*,  $p < 0.05$  versus vehicle ( $n = 6$ ). F, transcript levels of MMP-2 as determined by qPCR in retinas from OIR mice injected with either vehicle or Pifithrin- $\alpha$ . The data shown are the means  $\pm$  S.E. of three determinations each performed in triplicate. \*,  $p < 0.05$  versus vehicle ( $n = 6$ ). G, p53 enrichment of the endogenous MMP-2 promoter in OIR eyes previously injected with either vehicle or Pifithrin- $\alpha$ . Immunoprecipitated DNA was quantified by qPCR. \*\*,  $p < 0.01$  ( $n = 3$ ).

molecules and growth factors, cytokines, proteases, and other related proteins by virtue of its ECM-like structural features and its multifaceted cellular activities, including modulation of cell motility, adhesion, proliferation, predis-

position to apoptosis, and production of endothelial basement membrane components (48, 49). As such, this molecule is a prime candidate for the modulation of blood vessel formation and regeneration during development and disease.

In this study, we have uncovered novel functional properties of CTGF/CCN2 in retinal angiogenesis. First, examination of the vascular implications of CTGF/CCN2 expression, or lack thereof, during development and in response to hyperoxic injury showed a close correlation in topography and timing between CTGF/CCN2 gene expression and spatial distribution and expansion of retinal vessels. We found that development of the mouse retinal vasculature was concomitant with a progressive, time-dependent increase of CTGF/CCN2 levels and that suppression of CTGF/CCN2 expression or activity rather delayed normal expansion of the superficial capillary plexus to the edge of the retina. Under normal conditions, the retinal vasculature grows outwardly in a concentric manner in response to a chemotactic gradient of PDGF-A and VEGF previously deposited in the ECM by astrocytes, and the evolving retinal trees are then allowed to adapt and remodel by means of several biological stimuli (50–52). Because angiogenic stimuli such as VEGF and PDGF are potent inducers of the expression of CTGF/CCN2, which itself regulates migration and adhesion of astrocytes and endothelial cells (53, 54), it is conceivable that reduced levels of CTGF/CCN2, at least temporarily, compromised blood vessel sprouting and patterning. However, whether and how CTGF/CCN2 affects the branching “decisions” of blood vessels, which include cell proliferation, guided migration, tubulogenesis, vessel fusion, and pruning, is unknown. This process is dependent on selection and function of tip and stalk cells and the underlying regulation by the combined signaling of Notch and Wnt pathways that are critical for producing a mature retinal vascular system that is neither suffused by ectopic branches nor too sparse. CTGF/CCN2 may play an important role in this process by virtue of its known ability to integrate and modulate signals of both Notch and Wnt signaling pathways through either direct physical interaction with their components or regulation of *Notch* downstream genes (20). Further *in vivo* studies are needed to test the regulatory relationship between CTGF/CCN2 and guidance molecules responsible for vascular patterning.

Meanwhile, our data further showed that fluctuations of CTGF/CCN2 gene expression as a result of hyperoxic injury and ischemic response are important determinant of the degree and severity of retinal neovascularization. As shown in Figs. 1 and 3, CTGF/CCN2 protein localized within neovascular tufts formed in the ischemic retina, and fluctuations of CTGF/CCN2 levels occurred in parallel with those of VEGF, a major factor driving the formation of neovascular tufts. There are two potential molecular implications of these observations as follows. 1) There is a direct mutual regulatory relationship between VEGF and CTGF/CCN2 in the retina. Previous studies have indeed shown that VEGF is a potent activator of the CTGF/CCN2 gene primarily through binding to its high affinity receptors, Flt1 and KDR/Flk1, and activation of phosphatidylinositol 3-kinase (53). VEGF activates CTGF/CCN2 gene expression even at low concentrations (0.25 ng/ml) as commonly found in non pathological states. Thus, low levels of VEGF may have physiological effects by maintaining basal expression of CTGF/CCN2 that persists after completion of retinal network formation. Higher levels of VEGF, commonly associated with hypoxic and angiogenic states, induce aberrant

changes of CTGF/CCN2 gene expression compromising normal retinal cell growth and migration. Moreover, reduced levels of CTGF/CCN2 in the retina inhibit the expression of the VEGF gene as well (Fig. 4), suggesting a positive feedback loop involving a mutual coordinated regulation of the CTGF/CCN2 and VEGF genes. 2) Both CTGF/CCN2 and VEGF are direct targets of ischemic stimuli subsequent to the hyperoxic conditions in the retina. Previous studies have shown that hypoxia induces CTGF/CCN2 gene expression through the transcription factor *FoxO1*, whereas VEGF responsiveness is dependent on Hif-1 $\alpha$  in endothelial cells (55). Thus, the hypoxic conditions in the retina may contribute to the up-regulation of both genes although via distinct molecular pathways.

Interestingly, anti-CTGF/CCN2 treatment of OIR mice was antithetic to VEGF effects because inhibition of CTGF/CCN2 expression or activity remarkably decreased neovascularization. This suggests that CTGF/CCN2 potentiates and/or mediates, at least in part, the biological activity of VEGF. Functionally, CTGF/CCN2 is best known for its fibrotic and fibrogenic activities by virtue of its ability to stimulate fibrillar collagen and ECM protein gene expression in fibroblasts (22). Therefore, excessive production of CTGF/CCN2, commonly seen in proliferative retinopathies (56), was presumed to essentially cause scarring within fibrovascular membranes and fibrosis in the vitreo-retinal environment that can lead to membrane detachment and blindness. Furthermore, *in vitro* assays showed that CTGF/CCN2 may physically interact with VEGF and reduce the angiogenic activity of VEGF (57). These findings prompted other investigators to introduce the concept of a fibro-angiogenic switch that hypothetically occurs as excesses of CTGF/CCN2 suppress angiogenesis through formation of inactive CTGF/CCN2-VEGF complexes and activate fibrosis instead (58).

Interestingly, our study showed that excessively produced CTGF/CCN2 accumulates in the neovascular tufts formed in the ischemic retina, and inhibition of CTGF/CCN2 levels or activity significantly reduced retinal neovascularization but minimally affected hyperoxia-induced vaso-obliteration and intraretinal vascularization. Clearly, abnormally formed retinal vessels were specifically targeted by anti-CTGF/CCN2 therapy. Mechanistically, CTGF/CCN2 regulates neovascularization through modulation of the expression of MMP-2 that acts as its direct molecular target and downstream effector. Although the effects of CTGF overexpression on MMP-2 levels and activity may appear relatively modest (*i.e.* CTGF overexpression induced 4-, 3.1-, and 1.7-fold increases of mRNA and latent and active forms of MMP-2 respectively, following OIR), they nonetheless underscore the importance of small yet aberrant levels of MMP-2 in the formation of abnormal blood vessels in the retina. Indeed, OIR alone induced a mere 70% increase of MMP-2 gene expression and protein activity, yet inhibition of CTGF expression or activity suppressed the increase of MMP-2 levels associated with OIR and significantly reduced retinal neovascularization. A significant reduction of retinal neovascularization was similarly reported previously by Barnett *et al.* (59) in MMP-2 null mice and by MMP-2 inhibitors following OIR. There are other data in the literature supporting the argument that changes (as small as they sometimes might occur) of

## CTGF/CCN2 Function in Ischemic Retinopathy

the levels of key angiogenic factors, including MMP-2, affect the process of normal and abnormal blood vessel growth. In diabetic retinas, the study by Mohammad and Kowluru (60) showed that *MMP-2* gene expression increased by a mere 35% and that gelatinolytic activity of MMP-2 was increased by less than 2-fold. However, inhibition of MMP-2 in this model reduced capillary loss during diabetes. Suofu *et al.* (61) have shown that in the early ischemic brain both inactive and active MMP-2 levels were increased by less than 20%, yet inhibition of MMP-2 in this model significantly reduced the hemorrhagic incidence in the cortex. Meanwhile, other key angiogenic factors such as VEGF, a key determinant of vessel growth and permeability, increased by 2.5-fold at P17 in the OIR models as shown in Fig. 3C and by other groups (41). Bergers and Coussens (62) also reported that during the early development of solid tumors, VEGF, its receptors, and acidic FGF (all are important factors in retinal neovascularization as well) were either slightly increased or expressed at stable constitutive levels before and after angiogenesis begins, yet a synthetic inhibitor of VEGF signaling systematically inhibits angiogenesis and tumor growth. Taken together, these observations support our findings that inhibition of CTGF-induced *MMP-2* gene expression and activity were sufficient to tip the angiogenic balance in favor of neovessel growth inhibition.

MMP-2 belongs to a multigene family of secreted and cell surface-associated enzymes targeting for degradation other proteinases, clotting factors, chemotactic molecules, latent growth factors, and their binding proteins, cell surface receptors, and virtually every structural ECM protein (44). *MMP-2* expression and activity are particularly important during the initial steps of retinal neovascularization involving the degradation of the basement membrane and ECM components surrounding endothelial cells followed by migration and invasion of endothelial cells and formation of new vascular patterns. However, MMP-2 plays also an important role in the pathological degradation of nonstructural ECM blood vessel stabilizing proteins, including MCP-3, Fas ligand, and IGFBP-3. IGFBP-3, in particular, has vascular stabilizing effects by virtue of its ability to prevent oxygen-induced vaso-obliteration and regression and to reduce pre-retinal neovascularization in the mouse OIR model (63). Similarly, Fas ligand mediates remodeling of the hyperoxygenated retinal vasculature and leukostasis associated with OIR (64). Surprisingly, the CTGF/CCN2 protein is itself susceptible to degradation by MMP-2, which cleaves the hinge region between von Willebrand factor and TSP-1 domains leading to the generation of truncated CTGF/CCN2 forms that exhibit biological activities distinct from the intact protein (65). The levels of N-terminal fragment of the cleaved CTGF/CCN2 protein were found to be elevated in the vitreous of patients with active proliferative retinopathy suggesting that this truncated form plays a pathogenic role in retinal neovascularization (31). Thus, MMP-2 does not operate alone, but it promotes cascades, regulatory circuits, and networks that all dynamically interconnect to induce neovascularization. Future studies will use proteomic profiling techniques (*i.e.* degradomics) to uncover the diverse range of modulated molecules upstream and downstream in the CTGF- and MMP-2-mediated pathway.

Furthermore, our study identified a p53-binding site in the *MMP-2* promoter as critical for CTGF/CCN2-mediated *MMP-2* gene induction in OIR retinas. This finding is consistent with increased p53 levels concomitantly with those of MMP-2 in cells stimulated by CTGF/CCN2 and in the retina upon ectopic overexpression of CTGF/CCN2. The functional importance of the transcriptional requirement of p53 is confirmed by ChIP assay that showed increased occupancy of the p53-binding site on the chromatin of the endogenous *MMP-2* promoter and reduced enrichment of this site upon inhibition of CTGF expression or activity in OIR retinas. Ischemia-induced p53-dependent *MMP-2* gene expression was partially suggested by prior *in vitro* and *in vivo* studies that showed reduced ischemia-induced *MMP-2* gene transcription upon deletion of the *MMP-2* promoter region containing an RE-1-binding site for p53 and AP-1 transcription factors (66). Ischemia induced the expression and binding of c-Fos, c-Jun, JunB, FosB, and Fra2 to a noncanonical AP-1 site present in the *MMP-2* promoter and decreased binding of the transcriptional repressor JunD. In a model of hind limb ischemia, the *MMP-2* promoter was also enhanced by increased expression and binding of nuclear factor of activated T-cells-c2 (NFATc2) to consensus sequences within the first intron (67). In this model, deletion of either the 5' regulatory element (RE) region of the promoter or substitution of the first intron abolished ischemia-induced *MMP-2* transcription *in vivo*. The role of NFATc2 in CTGF/CCN2-induced *MMP-2* gene transcription in OIR model is not known. Our preliminary studies did not show significant changes in *NFAT2c* gene expression during transition from hyperoxic to ischemic phases of OIR or in CTGF/CCN2-stimulated retinal endothelial cells (data not shown). However, further studies are needed to ascertain the role, if any, of other transcription factors such as *NFAT2c* in the context of retinal neovascularization following hyperoxia.

The precise role played by p53 in retinal vessel remodeling is complex given the large number of p53-regulated genes, which include cell cycle checkpoints, apoptosis, and angiogenesis. A study by Yu *et al.* (68) has revealed substantial heterogeneity in the transcriptional responses to p53. In particular, more genes were found to be induced by high levels of p53 than by the lower endogenous levels of p53, which possibly reflects differences in the affinity of various promoters for p53, such that some are responsive only to high levels of p53. In the OIR model, CTGF/CCN2-induced p53 up-regulated the expression of the *MMP-2* gene. We also found that CTGF/CCN2 up-regulated, although to a lower extent than that of *MMP-2*, the thrombospondin-1 gene (data not shown), which is consistent with other studies that showed that loss of p53 function causes a drop of at least 20-fold in secreted thrombospondin-1 (68). However, it seems paradoxical that CTGF/CCN2 simultaneously up-regulates proangiogenic factors (*e.g.* MMP-2) as well as antiangiogenic ones (*e.g.* thrombospondin-1). One explanation is reflected by the study by Lee *et al.* (69) who showed that thrombospondin-1 induced MMP-2 activation through transcriptional and post-translational mechanisms. Thus, increased thrombospondin-1 expression would be relevant/compatible with the mechanisms of MMP-2 action in angiogenesis.



The findings reported here highlight the influence of CTGF/CCN2 on physiological and pathological angiogenesis in the retina. We showed that CTGF/CCN2 has direct effects on retinal vessel development and remodeling, which are important processes in vascular repair and adaptability to injurious stimuli. Although CTGF/CCN2 did not elicit a vaso-stabilizing effect in response to hyperoxia, it significantly contributed to pathological neovascularization associated with retinal ischemia by targeting various components of the neovascularization signaling network. Given that CTGF/CCN2 is a diffusible extracellular matrix protein, it is likely to affect the function and behavior of various cell types throughout the retinal layers. The utilization of mice with tissue-specific compounded deletion for a single or multiple genes (e.g. CTGF/CCN2, p53, MMP-2, and thrombospondin-1) will provide invaluable tools to tease out the regulatory relationships among CTGF/CCN2 and its downstream effectors and further our understanding of CTGF/CCN2 signaling pathways in the context of pathological angiogenesis associated with ischemic retinopathies.

*Acknowledgments*—We thank all members of the laboratory for their technical assistance and critical discussion and review of this work.

## REFERENCES

- Fleck, B. W., and McIntosh, N. (2008) Pathogenesis of retinopathy of prematurity and possible preventive strategies. *Early Hum. Dev.* **84**, 83–88
- Kalka, C., Asahara, T., Krone, W., and Isner, J. M. (2000) Angiogenesis and vasculogenesis. Therapeutic strategies for stimulation of postnatal neovascularization. *Herz* **25**, 611–622
- Quinn, G. E., Gilbert, C., Darlow, B. A., and Zin, A. (2010) Retinopathy of prematurity: an epidemic in the making. *Chin. Med. J.* **123**, 2929–2937
- Sapieha, P., Joyal, J. S., Rivera, J. C., Kermorvant-Duchemin, E., Sennlaub, F., Hardy, P., Lachapelle, P., and Chemtob, S. (2010) Retinopathy of prematurity. Understanding ischemic retinal vasculopathies at an extreme of life. *J. Clin. Invest.* **120**, 3022–3032
- Li Calzi, S., Neu, M. B., Shaw, L. C., Kielczewski, J. L., Moldovan, N. I., and Grant, M. B. (2010) EPCs and pathological angiogenesis. When good cells go bad. *Microvasc. Res.* **79**, 207–216
- McVicar, C. M., Colhoun, L. M., Abrahams, J. L., Kitson, C. L., Hamilton, R., Medina, R. J., Durga, D., Gardiner, T. A., Rudd, P. M., and Stitt, A. W. (2010) Differential modulation of angiogenesis by erythropoiesis-stimulating agents in a mouse model of ischaemic retinopathy. *PLoS. One* **5**, e11870
- Chen, C. C., and Lau, L. F. (2009) Functions and mechanisms of action of CCN matricellular proteins. *Int. J. Biochem. Cell Biol.* **41**, 771–783
- Liu, H., Yang, R., Tinner, B., Choudhry, A., Schutze, N., and Chaqour, B. (2008) Cysteine-rich protein 61 and connective tissue growth factor induce death and anoikis of retinal pericytes. *Endocrinology* **149**, 1666–1677
- Chaqour, B., Yang, R., and Sha, Q. (2006) Mechanical stretch modulates the promoter activity of the profibrotic factor CCN2 through increased actin polymerization and NF- $\kappa$ B activation. *J. Biol. Chem.* **281**, 20608–20622
- Hanna, M., Liu, H., Amir, J., Sun, Y., Morris, S. W., Siddiqui, M. A., Lau, L. F., and Chaqour, B. (2009) Mechanical regulation of the proangiogenic factor CCN1/CYR61 gene requires the combined activities of MRTF-A and CREB-binding protein histone acetyltransferase. *J. Biol. Chem.* **284**, 23125–23136
- Kireeva, M. L., Latinkić, B. V., Kolesnikova, T. V., Chen, C. C., Yang, G. P., Abler, A. S., and Lau, L. F. (1997) Cyr61 and Fisp12 are both ECM-associated signaling molecules. Activities, metabolism, and localization during development. *Exp. Cell Res.* **233**, 63–77
- Kunz, M., Moeller, S., Koczan, D., Lorenz, P., Wenger, R. H., Glocker, M. O., Thiesen, H. J., Gross, G., and Ibrahim, S. M. (2003) Mechanisms of hypoxic gene regulation of angiogenesis factor Cyr61 in melanoma cells. *J. Biol. Chem.* **278**, 45651–45660
- Twigg, S. M., Chen, M. M., Joly, A. H., Chakrapani, S. D., Tsubaki, J., Kim, H. S., Oh, Y., and Rosenfeld, R. G. (2001) Advanced glycosylation end products up-regulate connective tissue growth factor (insulin-like growth factor-binding protein-related protein 2) in human fibroblasts: a potential mechanism for expansion of extracellular matrix in diabetes mellitus. *Endocrinology* **142**, 1760–1769
- Abreu, J. G., Ketpura, N. I., Reversade, B., and De Robertis, E. M. (2002) Connective-tissue growth factor (CTGF) modulates cell signaling by BMP and TGF- $\beta$ . *Nat. Cell Biol.* **4**, 599–604
- Chen, C. C., Mo, F. E., and Lau, L. F. (2001) The angiogenic factor Cyr61 activates a genetic program for wound healing in human skin fibroblasts. *J. Biol. Chem.* **276**, 47329–47337
- Chen, C. C., and Lau, L. F. (2010) Deadly liaisons: fatal attraction between CCN matricellular proteins and the tumor necrosis factor family of cytokines. *J. Cell Commun. Signal.* **4**, 63–69
- Chintalapudi, M. R., Markiewicz, M., Kose, N., Dammai, V., Champion, K. J., Hoda, R. S., Trojanowska, M., and Hsu, T. (2008) Cyr61/CCN1 and CTGF/CCN2 mediate the proangiogenic activity of VHL-mutant renal carcinoma cells. *Carcinogenesis* **29**, 696–703
- Crean, J. K., Furlong, F., Mitchell, D., McArdle, E., Godson, C., and Martin, F. (2006) Connective tissue growth factor/CCN2 stimulates actin disassembly through Akt/protein kinase B-mediated phosphorylation and cytoplasmic translocation of p27(Kip-1). *FASEB J.* **20**, 1712–1714
- Hasan, A., Pokeza, N., Shaw, L., Lee, H. S., Lazzaro, D., Chintala, H., Rosenbaum, D., Grant, M. B., and Chaqour, B. (2011) The matricellular protein cysteine-rich protein 61 (CCN1/Cyr61) enhances physiological adaptation of retinal vessels and reduces pathological neovascularization associated with ischemic retinopathy. *J. Biol. Chem.* **286**, 9542–9554
- Katsube, K., Sakamoto, K., Tamamura, Y., and Yamaguchi, A. (2009) Role of CCN, a vertebrate-specific gene family, in development. *Dev. Growth Differ.* **51**, 55–67
- Kubota, S., and Takigawa, M. (2007) CCN family proteins and angiogenesis. From embryo to adulthood. *Angiogenesis* **10**, 1–11
- Leask, A., Parapuram, S. K., Shi-Wen, X., and Abraham, D. J. (2009) Connective tissue growth factor (CTGF, CCN2) gene regulation: a potent clinical bio-marker of fibroproliferative disease? *J. Cell Commun. Signal.* **3**, 89–94
- Arnott, J. A., Lambi, A. G., Mundy, C., Hendsi, H., Pixley, R. A., Owen, T. A., Safadi, F. F., and Popoff, S. N. (2011) The role of connective tissue growth factor (CTGF/CCN2) in skeletogenesis. *Crit. Rev. Eukaryot. Gene Expr.* **21**, 43–69
- Ivkovic, S., Yoon, B. S., Popoff, S. N., Safadi, F. F., Libuda, D. E., Stephenson, R. C., Daluiski, A., and Lyons, K. M. (2003) Connective tissue growth factor coordinates chondrogenesis and angiogenesis during skeletal development. *Development* **130**, 2779–2791
- Doherty, H. E., Kim, H. S., Hiller, S., Sulik, K. K., and Maeda, N. (2010) A mouse strain where basal connective tissue growth factor gene expression can be switched from low to high. *PLoS ONE* **5**, e12909
- Babic, A. M., Chen, C. C., and Lau, L. F. (1999) Fisp12/mouse connective tissue growth factor mediates endothelial cell adhesion and migration through integrin  $\alpha$ v $\beta$ 3, promotes endothelial cell survival, and induces angiogenesis *in vivo*. *Mol. Cell Biol.* **19**, 2958–2966
- Kuiper, E. J., Roestenberg, P., Ehlken, C., Lambert, V., van Treslong-de Groot, H. B., Lyons, K. M., Agostini, H. J., Rakic, J. M., Klaassen, I., Van Noorden, C. J., Goldschmeding, R., and Schlingemann, R. O. (2007) Angiogenesis is not impaired in connective tissue growth factor (CTGF) knock-out mice. *J. Histochem. Cytochem.* **55**, 1139–1147
- Shimo, T., Nakanishi, T., Nishida, T., Asano, M., Kanyama, M., Kuboki, T., Tamatani, T., Tezuka, K., Takemura, M., Matsumura, T., and Takigawa, M. (1999) Connective tissue growth factor induces the proliferation, migration, and tube formation of vascular endothelial cells *in vitro*, and angiogenesis *in vivo*. *J. Biochem.* **126**, 137–145
- Kuiper, E. J., van Zijderveld, R., Roestenberg, P., Lyons, K. M., Goldschmeding, R., Klaassen, I., Van Noorden, C. J., and Schlingemann, R. O.

- (2008) Connective tissue growth factor is necessary for retinal capillary basal lamina thickening in diabetic mice. *J. Histochem. Cytochem.* **56**, 785–792
30. Garcia Abreu, J., Coffinier, C., Larraín, J., Oelgeschläger, M., and De Robertis, E. M. (2002) Chordin-like CR domains and the regulation of evolutionarily conserved extracellular signaling systems. *Gene* **287**, 39–47
  31. Hinton, D. R., Spee, C., He, S., Weitz, S., Usinger, W., LaBree, L., Oliver, N., and Lim, J. I. (2004) Accumulation of NH<sub>2</sub>-terminal fragment of connective tissue growth factor in the vitreous of patients with proliferative diabetic retinopathy. *Diabetes Care* **27**, 758–764
  32. Grotendorst, G. R., and Duncan, M. R. (2005) Individual domains of connective tissue growth factor regulate fibroblast proliferation and myofibroblast differentiation. *FASEB J.* **19**, 729–738
  33. Yoon, P. O., Lee, M. A., Cha, H., Jeong, M. H., Kim, J., Jang, S. P., Choi, B. Y., Jeong, D., Yang, D. K., Hajjar, R. J., and Park, W. J. (2010) The opposing effects of CCN2 and CCN5 on the development of cardiac hypertrophy and fibrosis. *J. Mol. Cell. Cardiol.* **49**, 294–303
  34. Smith, L. E., Wesolowski, E., McLellan, A., Kostyk, S. K., D'Amato, R., Sullivan, R., and D'Amore, P. A. (1994) Oxygen-induced retinopathy in the mouse. *Invest. Ophthalmol. Vis. Sci.* **35**, 101–111
  35. Harendza, S., Pollock, A. S., Mertens, P. R., and Lovett, D. H. (1995) Tissue-specific enhancer-promoter interactions regulate high level constitutive expression of matrix metalloproteinase 2 by glomerular mesangial cells. *J. Biol. Chem.* **270**, 18786–18796
  36. Pi, L., Xia, H., Liu, J., Shenoy, A. K., Hauswirth, W. W., and Scott, E. W. (2011) Role of connective tissue growth factor in the retinal vasculature during development and ischemia. *Invest. Ophthalmol. Vis. Sci.* **52**, 8701–8710
  37. Gauthier, R., Joly, S., Pernet, V., Lachapelle, P., and Di Polo, A. (2005) Brain-derived neurotrophic factor gene delivery to Muller glia preserves structure and function of light-damaged photoreceptors. *Invest. Ophthalmol. Vis. Sci.* **46**, 3383–3392
  38. Kordower, J. H., Bloch, J., Ma, S. Y., Chu, Y., Palfi, S., Roitberg, B. Z., Emborg, M., Hantraye, P., Déglon, N., and Aebischer, P. (1999) Lentiviral gene transfer to the nonhuman primate brain. *Exp. Neurol.* **160**, 1–16
  39. Apte, R. S. (2010) Regulation of angiogenesis by macrophages. *Adv. Exp. Med. Biol.* **664**, 15–19
  40. Kociok, N., Radetzky, S., Krohne, T. U., Gavranic, C., and Jousen, A. M. (2006) Pathological but not physiological retinal neovascularization is altered in TNF-Rp55-receptor-deficient mice. *Invest. Ophthalmol. Vis. Sci.* **47**, 5057–5065
  41. Weidemann, A., Krohne, T. U., Aguilar, E., Kurihara, T., Takeda, N., Dorell, M. I., Simon, M. C., Haase, V. H., Friedlander, M., and Johnson, R. S. (2010) Astrocyte hypoxic response is essential for pathological but not developmental angiogenesis of the retina. *Glia* **58**, 1177–1185
  42. Viores, S. A., Xiao, W. H., Shen, J., and Campochiaro, P. A. (2007) TNF- $\alpha$  is critical for ischemia-induced leukostasis, but not retinal neovascularization nor VEGF-induced leakage. *J. Neuroimmunol.* **182**, 73–79
  43. Kowluru, R. A., and Kanwar, M. (2009) Oxidative stress and the development of diabetic retinopathy. Contributory role of matrix metalloproteinase-2. *Free Radic. Biol. Med.* **46**, 1677–1685
  44. Sternlicht, M. D., and Werb, Z. (2001) How matrix metalloproteinases regulate cell behavior. *Annu. Rev. Cell Dev. Biol.* **17**, 463–516
  45. Tronc, F., Mallat, Z., Lehoux, S., Wassef, M., Esposito, B., and Tedgui, A. (2000) Role of matrix metalloproteinases in blood flow-induced arterial enlargement: interaction with NO. *Arterioscler. Thromb. Vasc. Biol.* **20**, E120–E126
  46. Bian, J., and Sun, Y. (1997) Transcriptional activation by p53 of the human type IV collagenase (gelatinase A or matrix metalloproteinase 2) promoter. *Mol. Cell. Biol.* **17**, 6330–6338
  47. Di, Giovanni, S., and Rathore, K. (2012) p53-Dependent pathways in neurite outgrowth and axonal regeneration. *Cell Tissue Res.* **349**, 87–95
  48. Hall-Glenn, F., De Young, R. A., Huang, B. L., van Handel, B., Hofmann, J. J., Chen, T. T., Choi, A., Ong, J. R., Benya, P. D., Mikkola, H., Iruela-Arispe, M. L., and Lyons, K. M. (2012) CCN2/connective tissue growth factor is essential for pericyte adhesion and endothelial basement membrane formation during angiogenesis. *PLoS One* **7**, e30562
  49. Jun, J. I., and Lau, L. F. (2011) Taking aim at the extracellular matrix. CCN proteins as emerging therapeutic targets. *Nat. Rev. Drug Discov.* **10**, 945–963
  50. Sakimoto, S., Kidoya, H., Naito, H., Kamei, M., Sakaguchi, H., Goda, N., Fukamizu, A., Nishida, K., and Takakura, N. (2012) A role for endothelial cells in promoting the maturation of astrocytes through the apelin/APJ system in mice. *Development* **139**, 1327–1335
  51. Scott, A., Powner, M. B., Gandhi, P., Clarkin, C., Gutmann, D. H., Johnson, R. S., Ferrara, N., and Fruttiger, M. (2010) Astrocyte-derived vascular endothelial growth factor stabilizes vessels in the developing retinal vasculature. *PLoS One* **5**, e11863
  52. Watson, M. G., McDougall, S. R., Chaplain, M. A., Devlin, A. H., and Mitchell, C. A. (2012) Dynamics of angiogenesis during murine retinal development: a coupled *in vivo* and *in silico* study. *J. R. Soc. Interface* **9**, 2351–2364
  53. Suzuma, K., Naruse, K., Suzuma, I., Takahara, N., Ueki, K., Aiello, L. P., and King, G. L. (2000) Vascular endothelial growth factor induces expression of connective tissue growth factor via KDR, Flt1, and phosphatidylinositol 3-kinase-Akt-dependent pathways in retinal vascular cells. *J. Biol. Chem.* **275**, 40725–40731
  54. Wunderlich, K., Senn, B. C., Todesco, L., Flammer, J., and Meyer, P. (2000) Regulation of connective tissue growth factor gene expression in retinal vascular endothelial cells by angiogenic growth factors. *Graefes Arch. Clin. Exp. Ophthalmol.* **238**, 910–915
  55. Samarin, J., Wessel, J., Cicha, I., Kroening, S., Warnecke, C., and Goppelt-Strube, M. (2010) FoxO proteins mediate hypoxic induction of connective tissue growth factor in endothelial cells. *J. Biol. Chem.* **285**, 4328–4336
  56. He, S., Chen, Y., Khankan, R., Barron, E., Burton, R., Zhu, D., Ryan, S. J., Oliver, N., and Hinton, D. R. (2008) Connective tissue growth factor as a mediator of intraocular fibrosis. *Invest. Ophthalmol. Vis. Sci.* **49**, 4078–4088
  57. Inoki, I., Shiomi, T., Hashimoto, G., Enomoto, H., Nakamura, H., Makino, K., Ikeda, E., Takata, S., Kobayashi, K., and Okada, Y. (2002) Connective tissue growth factor binds vascular endothelial growth factor (VEGF) and inhibits VEGF-induced angiogenesis. *FASEB J.* **16**, 219–221
  58. Kuiper, E. J., Van Nieuwenhoven, F. A., de Smet, M. D., van Meurs, J. C., Tanck, M. W., Oliver, N., Klaassen, I., Van Noorden, C. J., Goldschmeding, R., and Schlingemann, R. O. (2008) The angio-fibrotic switch of VEGF and CTGF in proliferative diabetic retinopathy. *PLoS ONE* **3**, e2675
  59. Barnett, J. M., McCollum, G. W., Fowler, J. A., Duan, J. J., Kay, J. D., Liu, R. Q., Bingaman, D. P., and Penn, J. S. (2007) Pharmacologic and genetic manipulation of MMP-2 and -9 affects retinal neovascularization in rodent models of OIR. *Invest. Ophthalmol. Vis. Sci.* **48**, 907–915
  60. Mohammad, G., and Kowluru, R. A. (2010) Matrix metalloproteinase-2 in the development of diabetic retinopathy and mitochondrial dysfunction. *Lab. Invest.* **90**, 1365–1372
  61. Suofu, Y., Clark, J. F., Broderick, J. P., Kurosawa, Y., Wagner, K. R., and Lu, A. (2012) Matrix metalloproteinase-2 or -9 deletions protect against hemorrhagic transformation during early stage of cerebral ischemia and reperfusion. *Neuroscience* **212**, 180–189
  62. Bergers, G., and Coussens, L. M. (2000) Extrinsic regulators of epithelial tumor progression. Metalloproteinases. *Curr. Opin. Genet. Dev.* **10**, 120–127
  63. Chang, K. H., Chan-Ling, T., McFarland, E. L., Afzal, A., Pan, H., Baxter, L. C., Shaw, L. C., Caballero, S., Sengupta, N., Li Calzi, S., Sullivan, S. M., and Grant, M. B. (2007) IGF binding protein-3 regulates hematopoietic stem cell and endothelial precursor cell function during vascular development. *Proc. Natl. Acad. Sci. U.S.A.* **104**, 10595–10600
  64. Ishida, S., Yamashiro, K., Usui, T., Kaji, Y., Ogura, Y., Hida, T., Honda, Y., Oguchi, Y., and Adamis, A. P. (2003) Leukocytes mediate retinal vascular remodeling during development and vaso-obliteration in disease. *Nat. Med.* **9**, 781–788
  65. Dean, R. A., Butler, G. S., Hamma-Kourbali, Y., Delbé, J., Brigstock, D. R., Courty, J., and Overall, C. M. (2007) Identification of candidate angiogenic inhibitors processed by matrix metalloproteinase 2 (MMP-2) in cell-based proteomic screens: disruption of vascular endothelial growth factor (VEGF)/heparin affinity regulatory peptide

- (pleiotrophin) and VEGF/connective tissue growth factor angiogenic inhibitory complexes by MMP-2 proteolysis. *Mol. Cell. Biol.* **27**, 8454–8465
66. Bergman, M. R., Cheng, S., Honbo, N., Piacentini, L., Karliner, J. S., and Lovett, D. H. (2003) A functional activating protein 1 (AP-1) site regulates matrix metalloproteinase 2 (MMP-2) transcription by cardiac cells through interactions with JunB-Fra1 and JunB-FosB heterodimers. *Biochem. J.* **369**, 485–496
67. Lee, J. G., Dahi, S., Mahimkar, R., Tulloch, N. L., Alfonso-Jaume, M. A., Lovett, D. H., and Sarkar, R. (2005) Intronic regulation of matrix metalloproteinase-2 revealed by *in vivo* transcriptional analysis in ischemia. *Proc. Natl. Acad. Sci. U.S.A.* **102**, 16345–16350
68. Yu, J., Zhang, L., Hwang, P. M., Rago, C., Kinzler, K. W., and Vogelstein, B. (1999) Identification and classification of p53-regulated genes. *Proc. Natl. Acad. Sci. U.S.A.* **96**, 14517–14522
69. Lee, T., Esemuede, N., Sumpio, B. E., and Gahtan, V. (2003) Thrombospondin-1 induces matrix metalloproteinase-2 activation in vascular smooth muscle cells. *J. Vasc. Surg.* **38**, 147–154